Babes-Bolyai University, Faculty of Chemistry and Chemical Engineering,
Department of Chemistry

PhD Thesis Abstract

Lidia POP

Development of smart molecular building blocks for self-assembled networks MOFs and COFs

Scientific advisor

Prof. Dr. Ion Grosu

Cluj-Napoca
2016

Babes-Bolyai University, Faculty of Chemistry and Chemical Engineering,
Department of Chemistry

PhD Thesis Abstract

Lidia POP

Development of smart molecular building blocks for self-assembled networks MOFs and COFs

Defense 07th June 2016

Specialty: Organic Chemistry

Supramolecular Organic and Organometallic Chemistry Centre

Committee Members:

President:	**Prof. Dr. Cristian SILVESTRU**	Babes-Bolyai University, Cluj-Napoca, Romania
Reviewers:	**Assoc. Dr. Niculina D. HĂDADE**	Babes-Bolyai University, Cluj-Napoca, Romania
	Prof. Dr. Marius ANDRUH	University of Bucharest, Bucharest, Romania
	D.R. Mihail BĂRBOIU	European Membrane Institute, Montpellier, France

Scientific advisor: **Prof. Dr. Ion Grosu** Babes-Bolyai University, Cluj-Napoca, Romania

Cluj-Napoca
2016

General Contents

Keyworks:

Covalent Organic Frameworks,
Metal Organic Frameworks,
Tetraphenyladamantane, 9,9’-Spirobifluorene, Hydrogen Bonding

General Introduction

In the last four decades, the supramolecular chemistry, defined as "*the chemistry beyond the molecule*" has witnessed an important development[1] in the construction of complex, self-assembled chemical systems built from simple molecular subunits.

This thesis presents the results in the design, synthesis, structural analysis and investigation of the chemical and supramolecular proprieties of new tetraphenyladamantane and 9,9' spirobifluorene based ligands as well as their application in the construction of Metal–Organic Frameworks (MOFs), Covalent Organic Frameworks (COFs) and hydrophobic or hydrogen bonding self-assembled supramolecular architectures.

The PhD thesis is structured in six chapters. Unless otherwise stated, the topics addressed in this work were carried out within the Supramolecular Organic and Organometallic Chemistry Centre, the Organic and Supramolecular Chemistry Group, led by professor Ion Grosu.

Chapter I, entitled **„Covalent Organic Frameworks (COFs) based on tetrahedral and tetragonal ligands: from synthesis to applications''** describes the results in the synthesis and characterization of new COFs obtained from tetrafunctionalized ligands with tetrahedral or tetragonal disposition of the substituents. These ligands have the 9,9'-spirobifluorene or tetraphenyladamantane as central units.

Chapter II, entitled **„Self-Assembled Solid-State Networks with of 9,9′-Spirobifluorenes units''** shows a new synthetic strategy for convenient access to 3,3',6,6'-tetrasusbtituted 9,9'-spirobifluorene with tetrahedral orientation of the substituents and further decoration with various functional groups (*i.e.* -I, ethynyl, 4-Py, -CN, -CHO, $-NH_2$,-COOH, $-NO_2$). In addition, the solid state self-assembling properties of some of these ligands, driven by hydrophobic interactions, are discussed.

Chapter III, entitled **„New Nucleobases Decorated Tetragonal and Tetrahedral Ligands''** presents as element of innovation the synthesis of new tetrapodands with 1,3,5,7-tetraphenyladamantane and 9,9'–spirobifluorene central units, decorated with

[1] Lehn, J.-M.*Chem. Soc. Rev.* **2007**, *36*, 151-160.

nucleobases through a „click" reaction. These tetrapodants are interesting building blocks for the construction of hydrogen bonding or metal-ion directed 2D and 3D supramolecular architectures. All structures were fully characterised by Nuclear Magnetic Resonance Spectroscopy (1D: ^{1}H-NMR, ^{13}C-NMR and 2D-COSY) and High Resolution Mass Spectrometry (HRMS).

Chapter IV, entitled **„Metal Organic Frameworks (MOFs) based on tetrahedral and tetragonal ligands''** presents our results regarding the design, synthesis, structural analysis and proprieties of tetraphenyladamantane and 9,9' - spirobifluorene ligands with tetrahedral and tetragonal geometries as well as their applications as building blocks for the obtaining of Metal–Organic Frameworks(MOFs) with improved proprieties.

Chapter V, entitled **„Charge-Assisted Hydrogen Bonding Self-Assembly of bis-amidine -dicarboxylic acids complexes''** describes the Charge-Assisted Hydrogen Bonding (CAHB) association of diamidine derivatives with aromatic dicarboxylic and disulfonic acids. These associations were studied both in solution and solid state. Interestingly, the solid state structures revealed the formation of macrocycles of various sizes and shapes.

Finally, Chapter VI includes the experimental procedures and the structural characterisation of all newly synthesized compounds described in this work.

Chapter I. Covalent Organic Frameworks (COFs) based on tetrahedral and tetragonal ligands: from synthesis to applications

I.1 Introduction

The research in the field of COFs materials is a continuous challenge mainly due to the difficulties encountered in the synthesis of crystalline 3D networks but also because of their numerous applications. Therefore, in this chapter we focus on the preparation of new COFs, also named porous organic polymers (POPs). Thus, we used ligands with tetrahedral or tetragonal geometry having adamantane and 9,9'-spirobifluorene as central units (**Figure 1**). In order to obtain these polymers we used either acetylenic or Sonogashira coupling reactions.

An important target of our study was investigation of the gas adsorption properties of the newly synthesized materials as well as their utility as catalysts. Physicochemical characterization was carried out by spectroscopic methods FT-IR, X-ray diffractometry (XRD) and surface analysis while the porosity was determined using BET method. The stability of the powders was determined by thermal analysis, by simultaneous Thermogravimetric (TG) and Differential Thermal Analysis (DTA). All measurements were performed in collaboration with the ,,Catalysts and Catalytic Processes'' Research Group coordinated by professor Vasile PÂRVULESCU at the University of Bucharest.

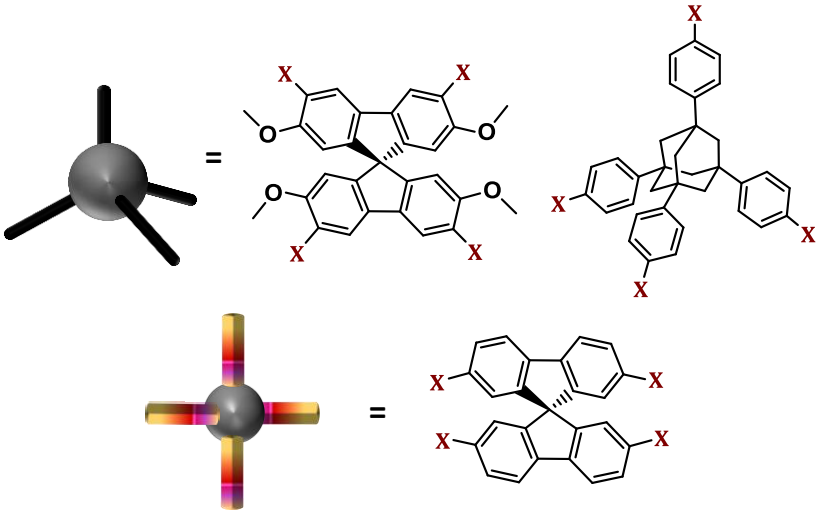

Figure 1. General structures of the tetraphenyladamantane and 9, 9' spirobifluorene ligands

I.3 Results and discussions

I.3.1 Synthesis of the ligands

I.3.1.1 9, 9'-Spirobifluorene based ligands

9,9'-Spirobifluorene derivatives are interesting molecular targets with a central tetrahedral C atom[2] similar with the tetrasubstituted methane,[3] silanes or adamantane derivatives.[4] 9,9'-Spirobifluorene unit can be decorated with a large variety of functional groups, using the usually encountered methods for the derivatization of the aromatic compounds.[5] The large majority of the reported derivatives with spirobifluorene core exhibit two or four identical or different substituents.

Their self-assembling behaviour is strongly related to the nature and position of the substituents on the aromatic backbone of the spirobifluorene platform. **(Figure 2)**

Disposal of the substituents in 2,2',7,7'-tetrasubstituted 9,9'-spirobifluorenes (**Figure 2**, **E**) reveal a tetragonal arrangement along two axes, the plans obtained with these axes and the spiro carbon atom being perpendicular. The 3,3',6,6'-

[2](a) Xie, L.-H.; Liang, J.; Song, J.; Yin, C.-R.; Huang, W. *Curr. Org. Chem.* **2010**, *14*, 2169-2195; (b) Wong, K.-T.; Ku, S.-Y.; Cheng, Y.-M.; Lin, X.-Y.; Hung, Y.-Y.; Pu, S.-C.; Chou, P.-T.; Lee, G.-H.; Peng, S.-M. *J. Org. Chem.* **2006**, *71*, 456–465; (c) Xiao, H.; Yin, H.; Zhang, X.; *Org. Lett*. **2012**, *14*, 5282–5285; (d) Schmidt, J.; Werner, M.; Thomas, A. *Macromolecules* **2009**, *42*, 4426–4429.

[3](a) Wuest, J. D.; *Chem. Commun*. **2005**, 5830–5837. (b) Chun, J.; Kang, S.; Park, N.; Park, E. J.; Jin, X.; Kim, K.-D.; Seo, H. O.; Lee, S. M.; Kim, H. J.; Kwon, W. H.; Park, Y.-K.; Kim, J. M.; Kim, Y. D.; Son, S. U. *J. Am. Chem. Soc*. **2014**, *136*, 6786-6789. (c) Yuan, D.; Lu, W.; Zhao, D.; Zhou, H.-C. *Adv. Mater*. **2011**, *23*, 3723–3725. (d) Dong, J.; Liu, Y.; Cui, Y. *Chem. Commun*. **2014**, *50*, 14949–14952. (e) Beaudoin, D.; Maris, T.; Wuest, J. D. *Nat. Chem.* **2013**, *5*, 830–834; (f) Muller, T.; Brase, S. *RSC Adv*, **2014**, *4*, 6886-6907. (g) Moon, S.-Y.; Mo, H.-R.; Ahn, M.-K.; Bae, J.-S.; Jeon, E.; Park, J.-W. *Polym. Chem.* **2013**, *51*, 1758–1766. (h) Zhu, X.; Tian, C.; Jin, T.; Wang, J.; Mahurin, S. M.; Mei, W.; Xiong, Y.; Hu, J.; Feng, X.; Liu, H.; Dai, S. *Chem. Commun*. **2014**, *50*, 15055–15058. (i) Stobe, C.; Seto, R.; Schneider, A.; Lützen, A. *Eur. J. Org. Chem*. **2014**, *29*, 6513–6518. (j) Tian, J.; Ding, Y.-D.; Zhou, T.-Y.; Zhang, K.-D.; Zhao, X.; Wang, H.; Zhang, D.-W.; Liu, Y.; Li, Z.-T. *Chem. -Eur. J*. **2014**, *20*, 575–584.

[4](a) Valera, S.; Taylor, J. E.; Daniels, D. S. B.; Dawson, D. M.; Arachchige, K. S. A.; Ashbrook, S. E.; Slawin, A. M. Z.; Bode, B. E. *J. Org. Chem*. **2014**, *79*, 8313−8323. (b) Schilling, C. I.; Plietzsch, O.; Nieger, M.; Muller, T.; Bräse, S. *Eur. J. Org. Chem*. **2011**, *9*, 1743–1754. (c) Fang, Q.; Gu, S.; Zheng, J.; Zhuang, Z.; Qiu, S.; Yan, Y. *Angew. Chem. Int. Ed*. **2014**, *53*, 2878–2882. (d) Schwenger, A., Gerlach, C.; Griesser, H.; Richert, C. *J. Org. Chem*. **2014**, *79*, 11558−11566.

[5](a) Yurkanis Bruice, P. *Organic Chemistry*, Pearson Education, Inc. London, Fifth edition, **2007**, 639-720; (b) Smith, M. B.; March, J. *Advanced Organic Chemistry*, Wiley, New Jersey, Sixth edition, **2007**, 657-750.

tetrasubstituted 9,9'spirobifluorenes derivatives (**Figure 2**, **F**) exhibit a tetrahedral orientation.

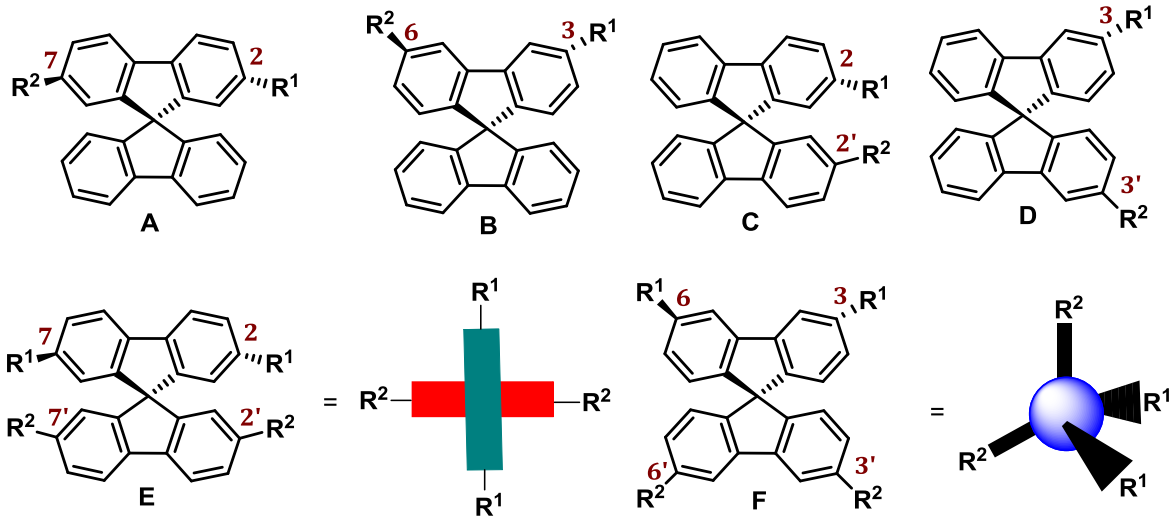

Figure 2. General formula of disubstituted (A-D) and tetrasubstituted (E and F) 9,9'-spirobifluorenes

Spirobifluorene **I** was obtained in a one-step synthesis using *o*-bromobiphenyl and fluorenone as starting materials.[6] (**Scheme 1)** The bromobiphenyl in the presence of magnesium/Et_2O (Grignard reaction) is transformed into the corresponding organomagnesium compound (Grignard reagent). The addition of this intermediate to the carbonyl group of fluorenone is followed by the formation of a carbocation which determines the closure of the spirane unit into the final compound via an aromatic electrophilic substitution.[7]

[6]Pei, J.; Ni, J.; Zhou, X.-H.; Cao, X.-Y.; Lai, Y.-H. *J .Org. Chem*. **2002**, *67*, 4924-4936.
[7]Grignard, V. *Compt*. *Rend*. *Acad. Sci*. **1900**, *130*, *1322-1325*.

Scheme 1. Synthetic Scheme for Preparation of Compounds **I** and **1**

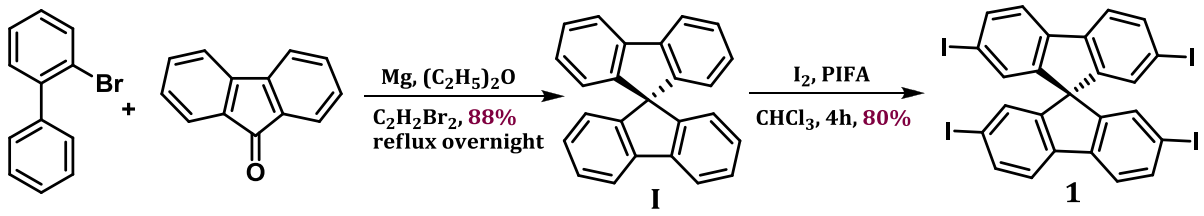

With compound **I** in our hand we moved to its decoration with various functional groups. This approach allowed the direct synthesis of 2,2',7,7' substituted derivatives, having a tetragonal orientation of the substituents. The key step was the regioselective synthesis of the tetraiodinated compound **1.** This was obtained in good yields by iodination reaction with I_2, in presence of bis(trifluoroacetoxy)iodo]benzene (PIFA) in $CHCl_3$, starting from spirobifluorene **I**.[8]

The synthesis of 3,3',6,6'-tetrasubstituted spirobifluorenes is far more challenging. Tetrahalogenated compound **1** in reaction with MeONa, CuI in DMF/MeOH yielded 2,2',7,7'-tetramethoxy-spirobifluorene **2.**[9] **(Scheme 2)**

Scheme 2. Synthetic Scheme for Preparation of Compound **2** from Compound **1**

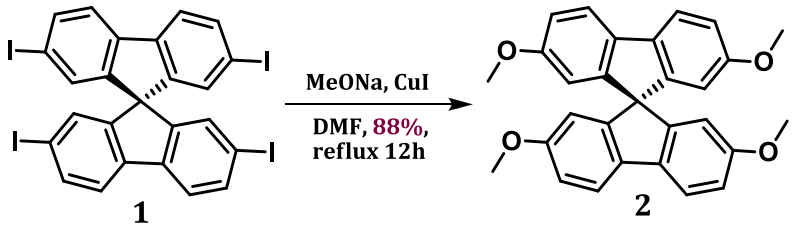

The iodination of **2**, in the same conditions (I_2, PIFA in $CHCl_3$) as for the synthesis of **1** regioselectively provided the target compound **3** in very good yield.[10] (**Scheme 3**)

[8]Salbeck, J.; Lupo, D. *Pat. Appl.* US20030111107A1, 2003

[9]Pop, L.; Dumitru, F.; Hădade, N. D.; van der Lee, A.; Barboiu, M.; Grosu, I. *Org. Lett.* **2015**, *17*, 3494-3497.

Scheme 3. Synthetic Scheme for Preparation of Compound **3** from Compound **2**

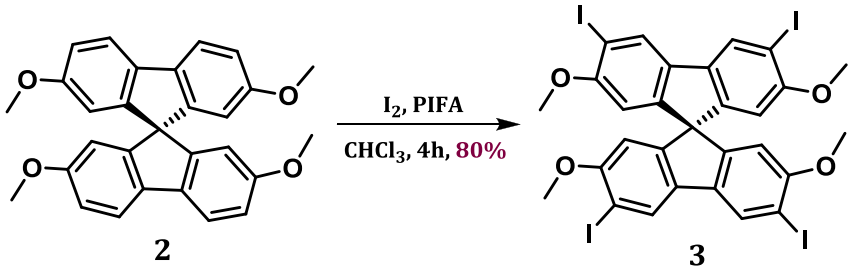

The reactivity of iodine atoms in **3** is similar to that observed for 2,2',7,7'-tetraiodo-9,9'-spirobifluorene.[10] The cross-coupling reaction of **3** with trimethylsilylacetylene (**Scheme 4**) was not considerably influenced by the methoxy groups in the substrate. The reaction conditions were slightly modified and the recorded yields were very good. In addition, the solubility of the starting material and products were improved in the case of compound **3**. The deprotection (KF, EtOH) of spirobifluorene **4** (synthesized through the reaction of **3** with trimethylsilyl-acetylene) gave the target tetraethynyl derivative **4.**[9]

Scheme 4. Synthetic Scheme for Preparation of Compounds **4** and **5** from Compound **3**

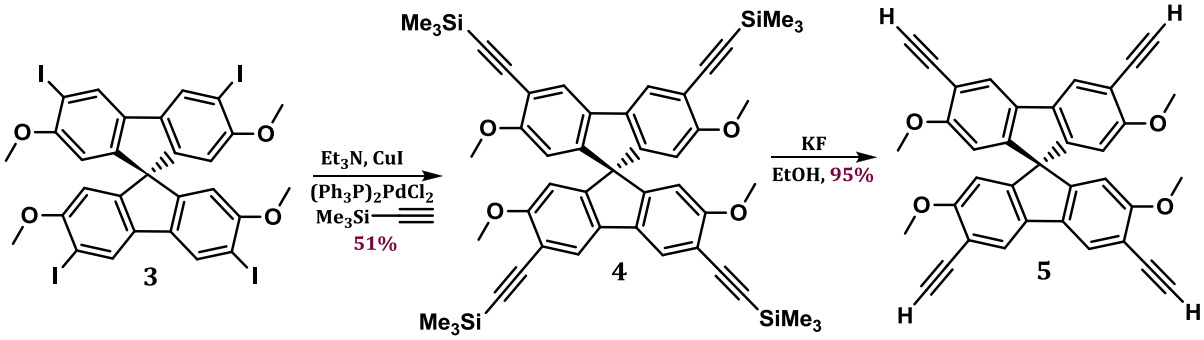

I.3.1.2 Adamantane based ligands

Another series of tetrahedral ligands was built up starting from the adamantane central unit decorated with four phenyl rings.

[10]Ren, H.; Tao, Q.; Gao, Z.; Liu, D. *Dyes Pigments,* **2012**, *94*, 136-142.

Tetraphenyladamantane **II** was obtained by Friedel Crafts reaction of 1-bromoadamantane with benzene, in presence of *tert*-butyl bromide and $AlCl_3$, following a previously described synthetic procedure.[11] **(Scheme 5)**.

Scheme 5. Synthetic Scheme for Preparation of Compound **II**

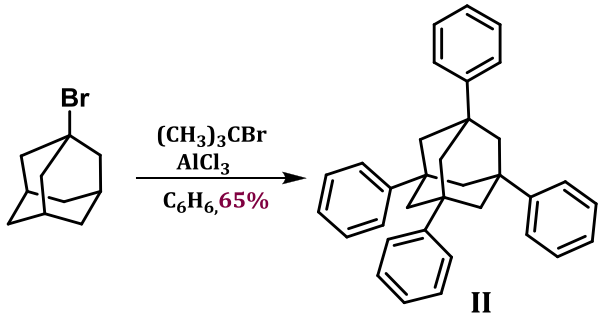

Compound **8** was obtained in a three steps synthesis: iodination of the tetraphenyladamantane, a Sonogashira cross-coupling with trimethylsilylacetylene and deprotection of the TMS groups.[12] (**Scheme 6**)

Scheme 6. Synthetic Scheme for Preparation of Compounds **6**, **7** and **8** from Compound **II**

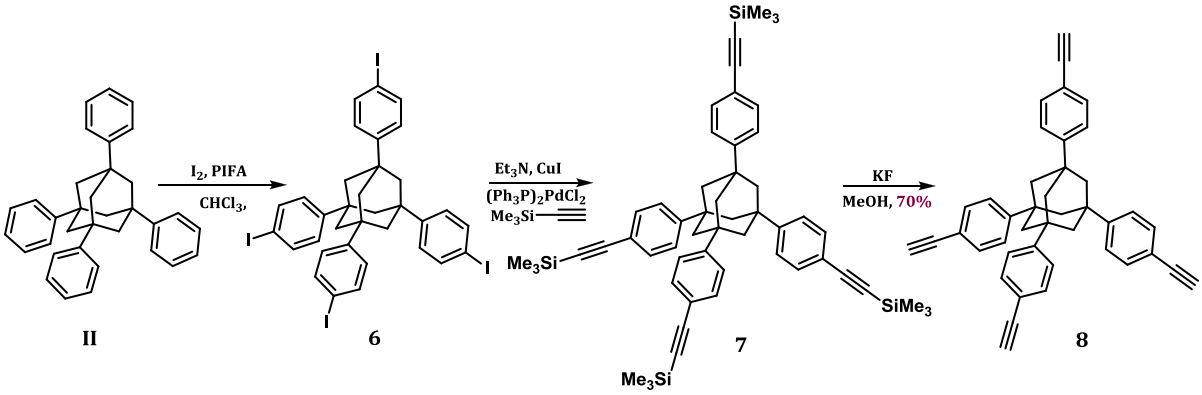

The ethynyl groups in compound **8** can further react in Sonogashira reactions thus opening the way to access a plethora of new compounds with tetrahedral geometry.

[11] Li, Q.; Rukavishnikov, A. V.; Petukhov, P. A.; Zaikova, T. O.; Keana, J. F. W. *Org. Lett*. **2002**, *4*, 3631-3634.

[12] Lu, W.; Yuan, D.; Zhao, D.; Schilling, C. I.; Plietzsch, O.; Muller, T.; Bräse, S.; Guenther, J.; Blümel, J.; Krishna, R.; Li, Z.; Zhou, H.-C. *Chem. Mater.* **2010**, *22*, 5964-5972.

I.3.2 COFs based on 9, 9'-spirobifluorene tetrahedral and tetragonal motifs: synthesis and applications

I.3.2.1 Synthesis of the COFs with spirobifluorene units

Once the monomer units **1**, **3** and **5** were synthesized, we turned our sights to the preparation of COFs with spirobifluorene units (**Figure 3**).

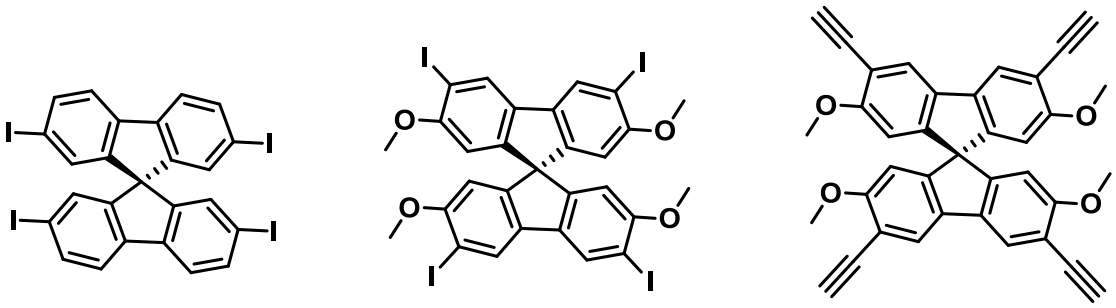

Figure 3. Structures of Tetragonal **1** and Tetrahedral **3, 5** monomers

Schemes **7-9** show the chemical structures and the chosen synthetic routes to obtain the COFs **9**, **12**, **13** and **15**.

Compound **9** was obtained by the acetylenic coupling reaction[13] starting from monomer **5**, which contains terminal acetylene groups.

The reaction was performed in dry DCM using CuI and tetramethylethylenediamine (TMEDA), under aerobe atmosphere, supplied by bubbling air into the reaction mixture. The reaction was stirred at room temperature for 12h, to obtain compound **9** as a precipitate. After filtration the obtained solid was washed with dichloromethane, methanol and water and dried, resulting in a pale yellow powder.

[13]Hay, A. S.*J. Org. Chem.* **1962**, *27* (9), 3320–3321.

Scheme 7. Synthetic Scheme for the Preparation of COF **9** Starting from **5**

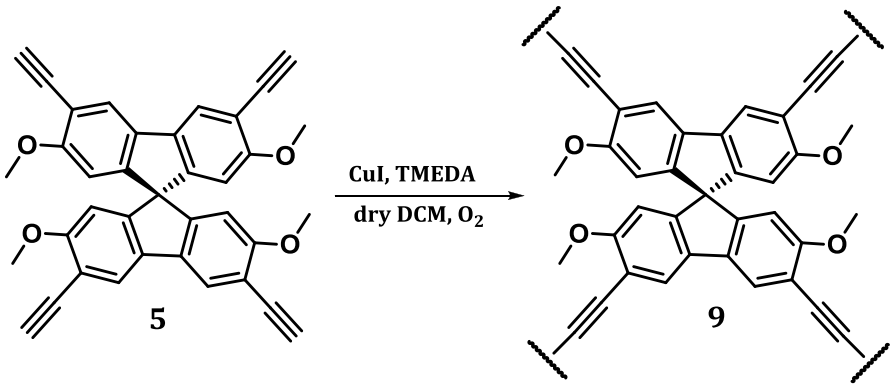

The synthetic strategy applied to obtain compounds **12** and **13** (**Scheme 10**) involved the Sonogashira coupling reactions between compounds **3** and 1,4-diethynylbenzene **10** or diethynyl-4,4'-biphenyl **11**, respectively (**Scheme 8**). The Sonogashira coupling was performed using the standard conditions:[12] $[(Ph_3P)_2PdCl_2]$ as palladium source and CuI co-catalyst into a mixture of toluene-triethylamine, at reflux for 48 hours, under inert atmosphere (argon). The compounds were obtained as brown solids in quantitative yields.

Scheme 8. Synthetic Scheme for the Preparation of COFs **12** and **13** Starting from **3**

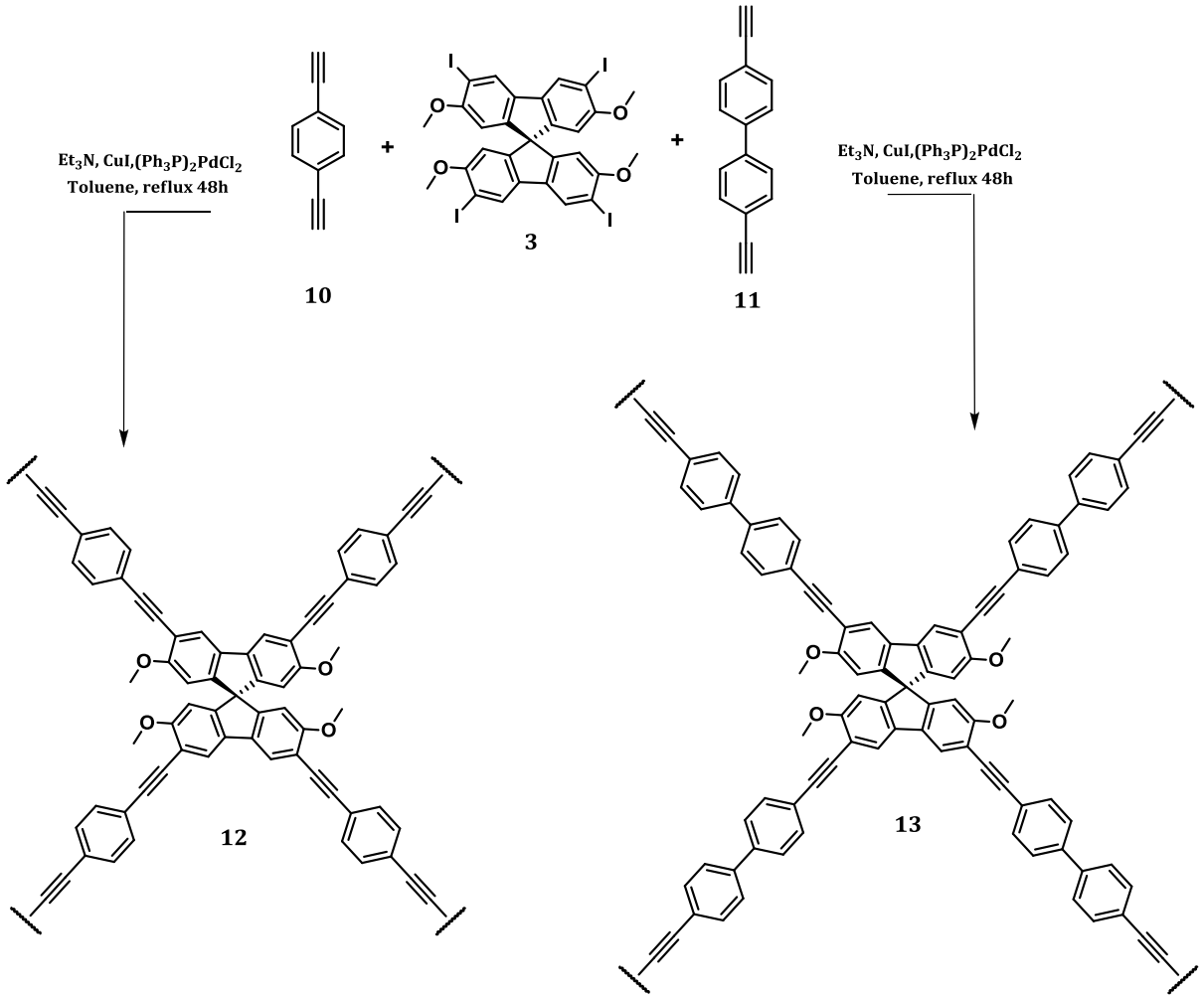

We also investigated the possibility to obtain 2D COFs with spirobifluorene units. These COFs were synthesized from 2,2',7,7'-tetraethynyl-9,9'-spirobifluorene derivative, through acetylenic coupling. The reaction yielded a complex mixture of compounds that could not be separated and purified. This was most probably due to the steric hindrance of the substituents in positions 2,7,2',7'. Thus, we considered the possibility to operate a correction of geometry (from tetragonal to tetrahedral) and to access 3D networks through Sonogashira coupling with 1,3-diethynylbenzene.

Therefore, compound **15** (**Scheme 9**) was prepared by Sonogashira cross-coupling of **1** with 1,3-diethynylbenzene **14**, following the same protocol as for COFs **12** and **13**.

Scheme 9. Synthetic Scheme for the Preparation of COF **15** Starting from **1**

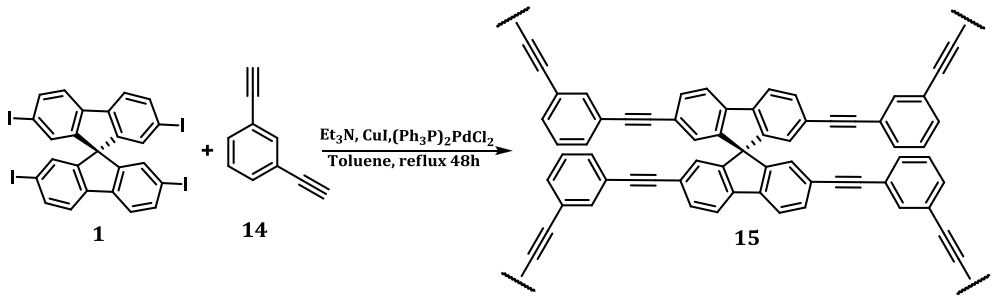

I.3.2.2 Textural and structural characterization of the COFs

Structural and textural characterization of COFs was performed by X-ray diffractometry, FT-IR, specific surface and porosity measurements as well as thermal analysis.

I.3.2.2.1 Adsorbtion-desorbtion isotherms

The textural characterization of COFs **9**, **12**, **13** and **15** was carried out by determination of nitrogen adsorption/desorption isotherms at -196 ^{0}C and the surface area has been calculated using the Langmuir method.[14]

The Langmuir surface area of materials, is presented in **Table 1.** Calculation of the pore size followed the Horwath−Kawazoe formalism for micropores. (**Table 1**)

COFs	Langmuir surface area (m^2g^{-1})	Horwath−Kawazoe pore size (Å)
9	**510**	**9.1**
12	**599**	**9.6**
13	**367**	**9.5**
15	**492**	**9.4**

Table 1. Langmuir surface area and Horwath-Kawazoe pore size of **9**, **12**, **13** and **15**

[14]Langmuir, I. *J. Am.Chem.Soc*. **1918**, *40*, 1361-1403.

I.3.2.2.2 Thermogravimetry Analysis-Differential Thermogravimetry Analysis (TG/DTA)

The thermogravimetrical analysis of these materials revealed a good thermal stability until 200°C for **9** and 300 °C for **12**, **13** and **15** with approximately 5% weight loss.

Higher temperatures led to one step mass loss for all the prepared materials that has been accompanied by several exothermal effects corresponding to the compound decomposition. Compound **9** decomposes almost entirely at 800 °C while **13** completely decomposes at 600°C. At 800°C materials **12** and **15** showed a weight loss of only 45% and 55%, respectively, showing better thermal stabilities. This fact could be correlated with the metal traces found in the material composition, as evidenced in the XRD patterns and further presented.

I.3.2.2.3 X-Ray Diffraction (XRD)

The XRD patterns of COFs **9** and **12** presents intense diffraction lines at 2θ= 25 and 49 (50), materials **13** and **15** have characteristic amorphous structures while **12** and **15** contains a small diffraction line at 41 2θ specific for (111) Pd crystallographic face.

I.3.3 COFs based on adamantane tetrahedral motifs: synthesis and applications

I.3.3.1 Synthesis of the COFs with tetraphenyladamantane units

To obtain compound **16**, we carried out an acetylene coupling reaction[13] using compound **8** in presence of CuI and TMEDA in dichloromethane, as solvent with air bubbling in solution.

Scheme 10. Synthetic Schemes for the Preparation of COF **16** Starting from **8**

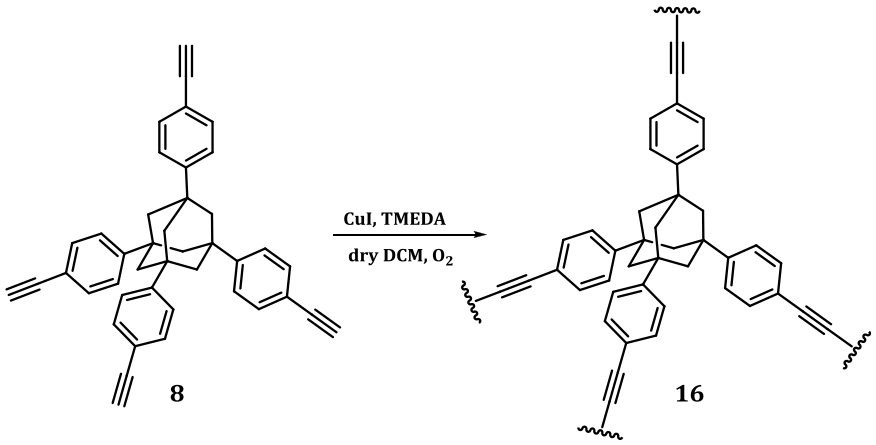

Tetraiodo derivative **6** was subjected to Sonogasira coupling reactions (**Schemes 11, 12**) with compounds **10** and **11**, under classic conditions, in the presence of triethylamine as base and $[(PPh_3)_2PdCl_2]$ and CuI as catalysts, to obtain COFs **17** and **18**. These COFs were obtained in quantitative yields and characterized by spectroscopic, surface and thermal analysis.

Scheme 11. Synthetic Schemes for the Preparation of COF **17** Starting from **6**

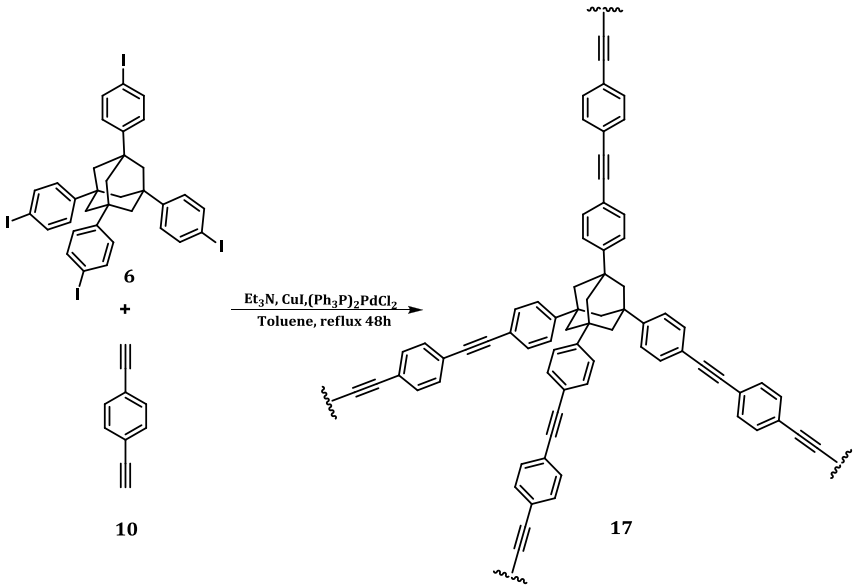

Scheme 12. Synthetic Schemes for the Preparation of COF **18** Starting from **6**

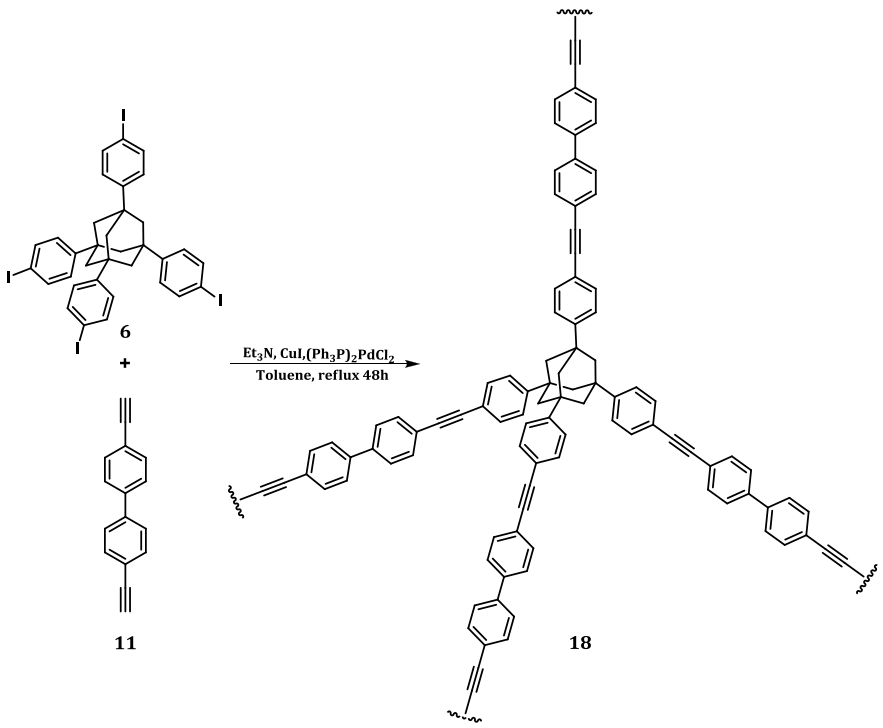

I.3.3.2 Textural and structural characterization of the COFs

I.3.3.2.1 Characterization of COFs 16 and 17

The characterisation of structure and properties of COFs **16** and **17** was carried out by measuring the adsorption and desorption isotherms of nitrogen at -196^{0}C, by Langmuir[14] and BET[15] (Brunauer-Emmett-Teller) methods that consists in the adsorption of krypton at liquid nitrogen liquid temperature (-196 ^{0}C) using programs for both micropores mesopoores and macropores .The surface area has been determined in accordance with the pore size and the composition of the pore walls. The surface areas determined for the two COFs using Langmuir method are 999m^2/g^{-1} for compound **16** and 379 m^2/g^{-1} for the compound **17**, respectively. In addition, the pores size distribution (*i.e.* diameter of the pores) for the two polymers were obtained using the model Barrett-Joyner-Halenda (BJH).[16] (**Table 2**)

[15]Brunauer S.; Emmett P. H.; Teller E. *J. Am. Chem. Soc*.**1938**, *60*, 309-319.
[16]Analytical Methods in Fine Particle Technologyî, Ed. Micromeritics Instrument Corporation, Norcross, **1997**, p. 81.

COFs	Langmuir surface area (m^2g^{-1})	BET surface area (m^2g^{-1})
16	999	744
17	379	281

Table 2. Langmuir and BET surface area of **16** and **17**

I.3.3.2.1 Characterization of the COF 18

In the case of the COF **18** we determined the thermal stability, the adsorption behaviour and, as catalyst support for Pd and Au, its catalytic activity in the hydrogenation reaction of *para*-nitrostyrene.

Pd and Au based catalysts were prepared in the same conditions, via the deposition-precipitation method. Moreover, for an accurate comparison, the Pd and Au supported on active carbon were prepared by the same procedure as for Pd and Au/COF **18**.

Table 3 presents the textural structural characteristics of the catalysts. For the calculation of the pores size, two methods, namely Horwath–Kawazoe[17] for micropores and BJH for mesopores[16] have been applied. Deposition of Pd or Au on COF **18** have not led to changes in the profile of the isotherms or in the calculated values for this material.

Sample	Langmuir surface area, m^2g^{-1}	BET surface area, m^2g^{-1}	Horwath−Kawazoe pore size, Å	BJH mesopore pore size, Å	Total pore volume, cm^3g^{-1}
18	774	577	8	40	0.35
Pd/18	756		8		
Au/18	745		8		

Table 3. Textural characteristics of the investigated catalysts (COF **18**, COF **18/Pd** and COF **18/Au**)

Representatives diffractograms of compound **18** showed two lines, at 41 and 47 2θ that are specific to the (111) and (200) Pd crystallographic facets. The presence of Pd in the material **18** was explained by the decomposition of $PdCl_2(PPh_3)_2$ (used

[17] Horvath, G.; Kawazoe, K. *J. Chem. Eng. Jpn*. **1983**, *16*, 470-475.

as Sonogashira catalyst for the preparation of **18**) to Pd metal, under the thermal reduction conditions[18]. Particle size was calculated using the Scherrer equation. Accumulation of Pd has resulted in particles of 10.3 nm, while the accumulation of Au resulted in particles of 9.6 nm. The XRD of C, Au/C and Pd/C catalyst indicated that the accumulation of Pd results in particle with sizes smaller than the XRD detection limit, while the particles obtained by deposition of Au on active carbon display similar sizes to those obtained in the case of **Au/18.**

The TEM (Transmission electron microscopy) picture of COF **18** showed spherical particles with average diameters of 1.7 nm. This material contains small amounts of Pd particles, incorporated into the material during the Sonogashira synthesis, which are highly dispersed. However, in the case of **Pd/18** 0.5wt% the size of particles increases at about 4.2 nm, after deposition of Pd.

The thermogravimetric (TG) analysis showed that COF **18** is thermally stable up to 300°C , when a loss of the weight of 2,7% was observed. Increase of the temperature at 300-600°C yielded a loss of weight of 91% accompanied by exothermal effects, corresponding to the decomposition of the compound. The resulted TG profile after addition of Pd indicated a similar thermal behaviour of **Pd/18** with material **18**. However, the DTA profile is in agreement with the elimination of small thermal effects in the range 300-600° C.

Catalytic activity

The catalytic activity of COF **18**, Au/**18** and Pd/**18** was evaluated in the hydrogenation of 4-nitrostyrene. (**Scheme 13**)

[18]Ishida, T.; Onuma, Y.; Kinjo, K.; Hamasaki, A.; Ohashi, H.; Honma, T.; Akita, T.; Yokoyama, T.;Tokunaga, M.; Haruta, M. *Tetrahedron*, **2014**, *70*, 6150-6155.

Scheme 13. Possible Hydrogenation Products in the Hydrogenation of *para*-Nitrotrostyrene

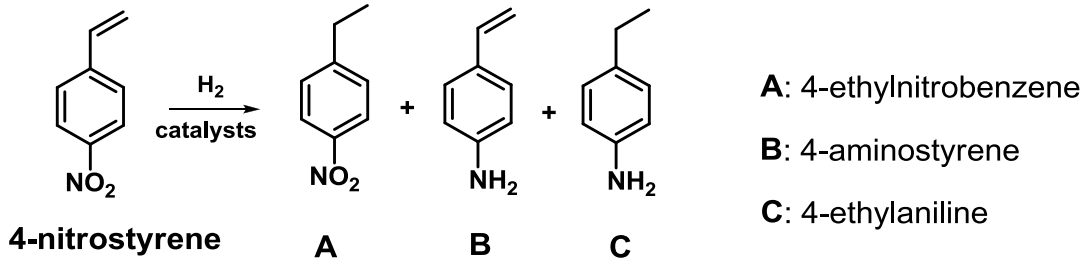

The reaction catalysed by COF **18** occurred in 20% conversation and total selectivity toward the formation of *para*-ethylnitrobenzene (A). Addition of Pd (0.5% by weight) to COF **18** resulted in a significant increase of activity (total conversion) preserving the selectivity for **A.** However, after 6 hours of reaction, the initiation of hydrogenation of the nitro group could be observed.

Another important factor, except for choosing the correct support and the reaction time, for chemoselective hydrogenation of 4-nitrostyrene is the selection of the solvent. For example, in polar solvents, the selectivity of the **Pd/18** was radically changed and only the total hydrogenation product (C) has been detected.

Hydrogenation of *para*-nitrostyrene with 0.5% Au (III)/**18** catalyst yielded similar results as in the case of Pd/**18** catalyst. However, reduction of the Au catalyst at Au (I)/**18** resulted in a loss of selectivity.

I.4 Conclusions

In conclusion, we described herein the synthesis of seven new COFs obtained from ligands with tetrahedral disposition of the substituents via Sonogashira cross-coupling or acetylenic coupling reactions.

The four monomers (**1**, **3**, **5**, **8**) used in of Sonogashira cross-coupling reactions have 9.9'-spirobifluorene or tetraphenyladamantane central units. The central core was functionalized with terminal reactive groups (ethynyl, iodine) following multistep synthetic procedures. The structure of these monomers was investigated by NMR Spectroscopy and Mass Spectrometry.

The physicochemical characterization of COFs was carried out by FT-IR and X-ray diffraction (XRD). Moreover, surface area and the porosity were determined by Langmuir and BET methods, respectively. The thermal stability of the particles was demonstrated by thermogravimetric TG-DTA analysis. In addition, for a complete

and full understanding of these materials the structures were investigated by imaging techniques (TEM)

The COF **18**, obtained in the Sonogashira cross-coupling of tetraiodotetra-phenyladamantane with diethynyl-4,4'-biphenyl, proved to have a very good thermal stability. This material has the property to adsorb large amounts of CO_2 and reduced quantities of H_2. Moreover, it proved to be a good catalyst, in terms of selectivity and conversion, for the hydrogenation of *p*-nitrostyrene to *p*-nitroethylbenzene. Deposition of active metals (*i.e.* Pd and Au) on COF **18** resulted in an increase of the catalytic activity and a tune of catalyst selectivity.

Chapter II. Self-Assembled Solid-State Networks with of 9,9′-Spirobifluorene units

II.1 Introduction

This chapter presents the development of a convenient and straightforward procedure to obtain 3,3',6,6'-tetrasubstituted-9,9'-spirobifluorene derivatives bearing tetrahedral-oriented reactive groups **Figure 4** (-I, ethynyl, 4-Py, -CN, -CHO, $-NH_2$,-COOH, $-NO_2$) starting from the already known 2,2',7,7'-tetraiodo-9,9'-spirobifluorene. Compounds characterisation was performed by NMR, HRMS, FT-IR, UV-Vis and, in some cases single crystal X-ray diffraction.

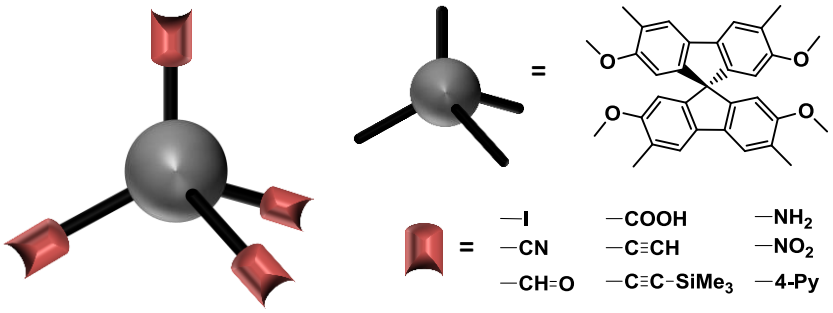

Figure 4. General chemical representation of 3,3',6,6'-tetrasubstituted-9,9'-spirobifluorene derivatives

II.3 Objective

Our target was to synthesize tetrahedral 2,2′,7,7′-tetramethoxy-3,3′,6,6′-substituted-9,9′-spirobifluorenes derivatives using methoxy (CH_3O-) *ortho*-directing groups in the 2,2′,7,7′ positions and further study of their self-assembling properties.

II.4 Results and discussions

Herein, we report a series of 2,2′,7,7′-tetramethoxy-3,3′,6,6′-substituted-9,9′spirobifluorenes **3-5/19-25** (substituents: -I, -CN, -NO_2, -CH=O, -COOH,-4-py, -NH_2, ethynyl). Four (-I, -CN, -NO_2 and ethynyl) of these compounds, were crystallized. Single- crystal molecular structures evidenced the formation of self-assembled molecular solids merely by weak hydrophobic interactions.

II.4.1 Synthesis of the ligands

The synthetic strategy employed as first step the quantitative transformation of 9,9′-spirobifluorene with I_2/bis[(trifluoroacetoxy)- iodo]benzene-PIFA in $CHCl_3$ into the tetraiodinated derivative **1**[8] **(see Scheme 1, Chapter 1).**

Next, the 2,2',7,7'-tetrametoxy-spirobifluorene **2** was obtained through the reaction of 2,2',7,7'-tetrahalogeno-spirobifluorene **1** with MeONa and CuI in DMF/MeOH.

The diiodinated **19** as well as the tetraiodinated **3** were obtained in similar conditions as compound **1**, according to the selected molar ratios of **2**: I_2: PIFA 1:1:1 and 1:2:2, respectively.[9] **(Scheme 14)** Structure assignment was achieved using ^1H, ^{13}C NMR and ROESY spectra.

Scheme 14. Synthetic Scheme for Preparation of Compounds **19, 3** from Compound **2**

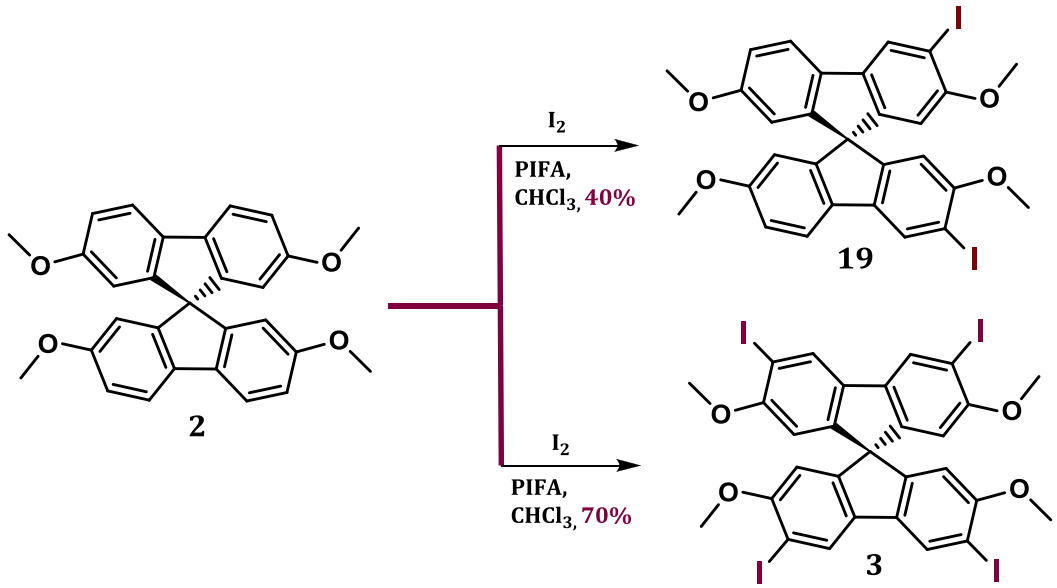

The tetracyano derivative **20** was obtained in good yield (79 %) starting from **3** (see **Scheme 3**, **Chapter I**) by classic nucleophilic aromatic substitution of iodine with CuCN in DMF.[9](**Scheme 15**).

Hydrolysis of the cyano groups, carried out by treatment of **20** with aqueous KOH in ethanol followed by acidulation with HCl, provided the tetracarboxy derivative **21**(75 % yield).[9] (**Scheme 15**)

Scheme 15. Synthetic Scheme for Preparation of Compounds **20** and **21** from Compound **3**

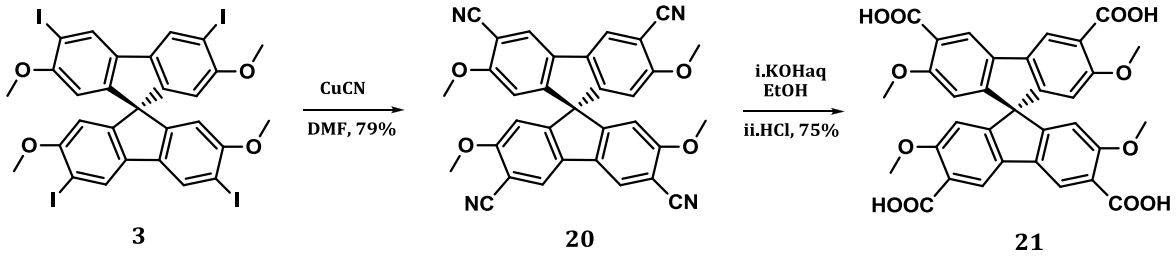

Tetraformyl derivative **22** was obtained in 40 % by treating compound **2** (see, **Scheme 2**, **Chapter I**) with Cl_2CHOCH_3, in presence of $TiCl_4$ as catalyst. (**Scheme 16**)

Scheme 16. Synthetic Scheme for Preparation of Compound **22** from Compound **2**

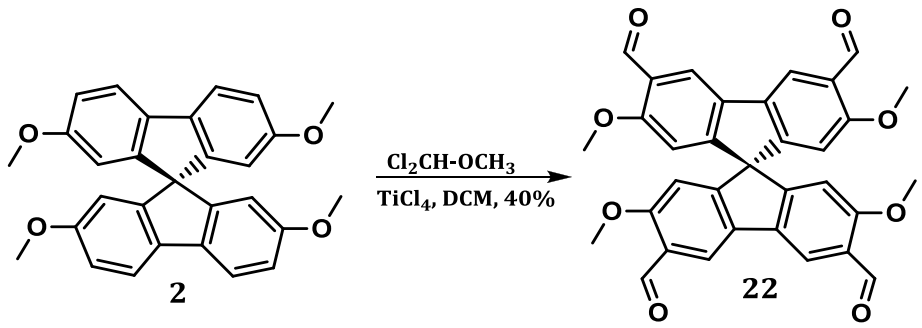

Nitration of **2** regioselectively provided, in very good yields (85 %), the tetranitroderivative **23. (Scheme 17)**

The reduction of the tetranitro derivative **23** with H_2, employing Pd/C as catalyst, led to the tetraamino compound **24** in very good yields (87 %). Thus, the 9,9'-spirobifluorene having the amino groups at the positions 3,3',6,6' was obtained in four steps, starting from the unsubstituted 9,9'-spirobifluorene **I** instead of the seven

steps procedure proposed by Wuest (see **Scheme 1**, **Chapter I**). In addition, we obtained considerably improved overall yields (65 % versus of 20 %).

Scheme 17. Synthetic Scheme for Preparation of Compounds **23** and **24** from Compound **2**

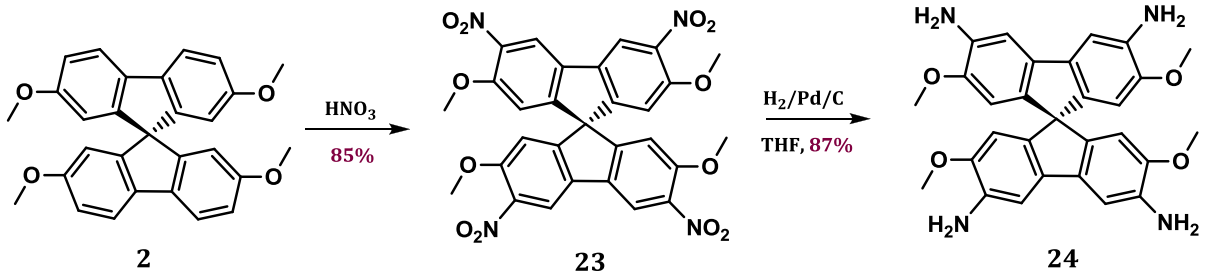

The Suzuki-Miyaura cross coupling reaction between compound **3** (**see Scheme 3**, **Chapter I**) and the less reactive 4-pyridyl boronic acid underwent in modest yields (**25**, 38 %).[9] (**Scheme 18**) However, the coupling reactions with more reactive boronic acids are expected perform better, thus leading to a wide variety of other tetrahedral tetraarylspirobifluorenes in better yields.

Scheme 18. Synthetic Scheme for Preparation of Compound **25** from Compound **3**

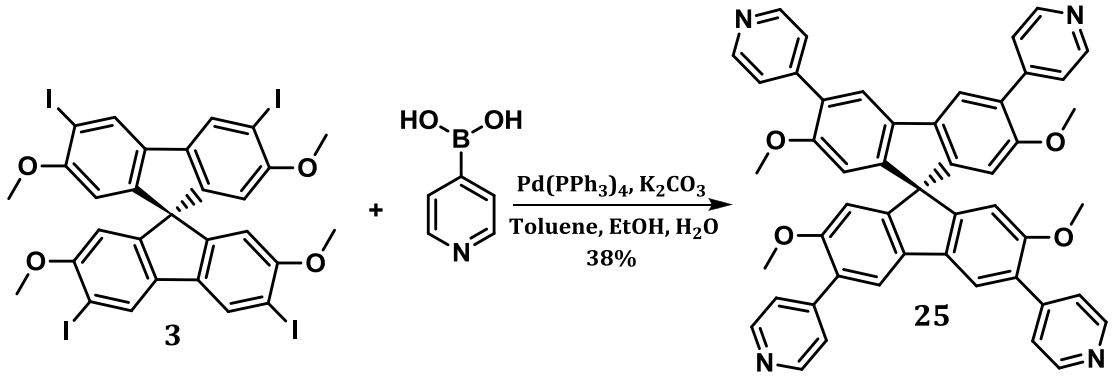

The structures of compounds **2-5/19-25** were confirmed by ^{1}H and ^{13}C NMR spectra, ES(+)-HRMS measurements and single-crystal X-ray diffractometry

II.4.2 Solid state molecular structures

The solid state molecular structures of compounds **3**, **5, 20** and **23 (Figure 5)** were determined using monocrystals obtained from mixtures of

dichloromethane/diethyl ether or dichloromethane/diisopropyl ether at room temperature.

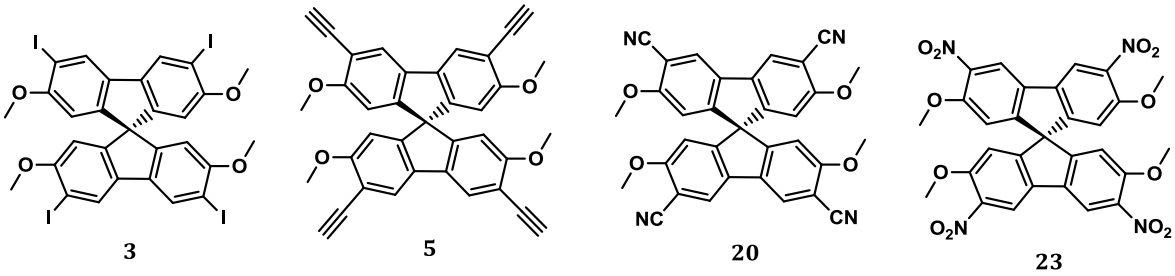

Figure 5

The single crystal molecular structures and the crystal packing are presented in **Figures 6-9**. In all structures the octasubstitutted spirobifluorene unit exhibits a slightly distorted tetrahedral geometry with angles varying between 100^0 and 118^0, while the dihedral angle between the fluorene rings range from 87.89^0 to 89.78^0. The angles distortions from the ideal sp^3-hybridization geometry around the central tetrahedral carbon atom most probably occur due to the strain imposed by the central five-membered ring as well as the indirect steric effects imposed by the variable crystal packing.

II.4.3 Self-assembling properties of compounds 3, 5, 20 and 23

The self-assembly of the monomeric units can form tetrameric and hexameric aggregates by symmetry expansion of the crystal cell. These shapes are triangular hexamers for **3**, **(Figure 6)**, extended hexagonal hexamers for **23**, **(Figure 7),** squared tetramers for **20 (Figure 8)** and star-type hexamers for **5** (**Figure 9)**.

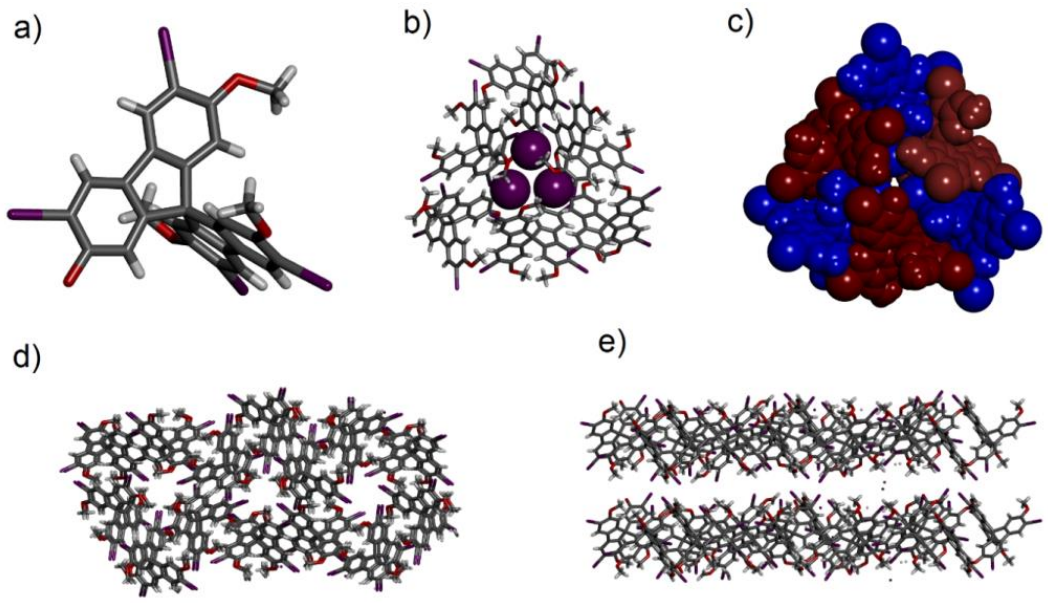

Figure 6. Crystal structure of **3** (a) and of the associated hexamers of $\mathbf{3}_6$ in stick (b) and CPK (c) representations; top (d) and side (e) view of the crystal packing of **3**.

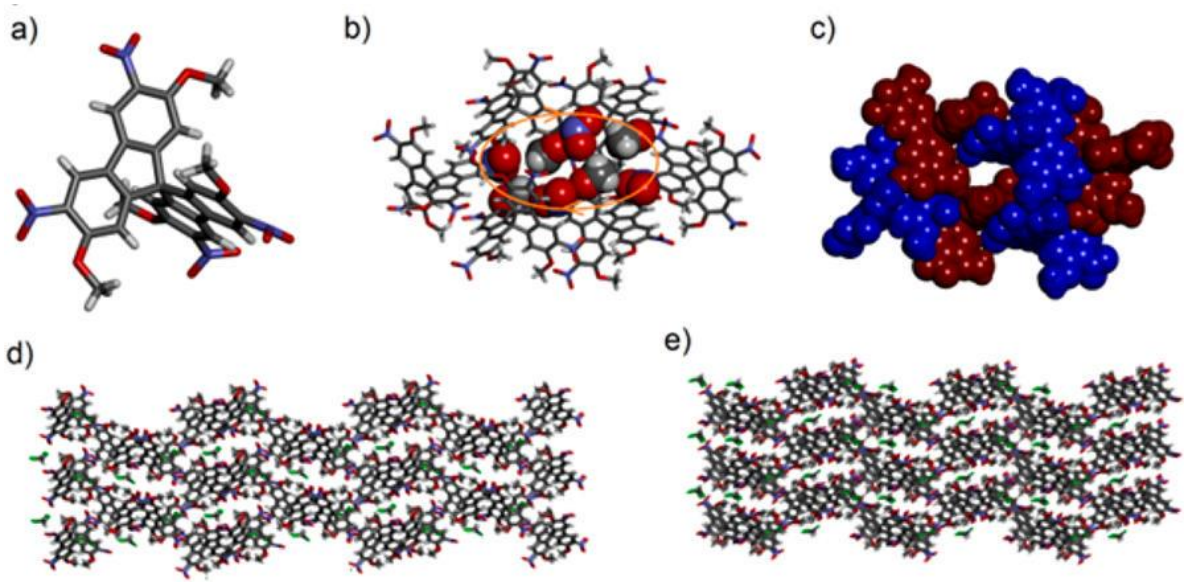

Figure 7. Crystal structure of **23** (a) and of the associated hexamers $\mathbf{23}_6$ in stick (b) and CPK (c) representations; top (d) and side view (e) of the crystal packing of **23**.

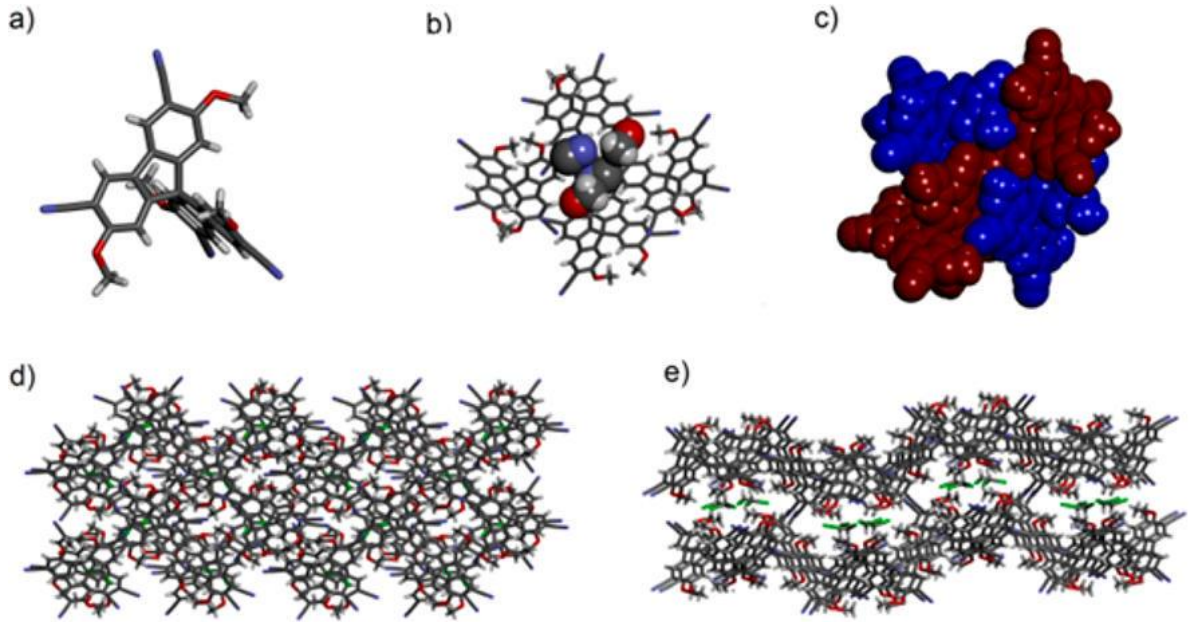

Figure 8. Crystal structure of **20** (a) and of the associated tetramers $\mathbf{20}_4$ in stick (b) and CPK (c) representations; top (d) and side view (e) of the crystal packing of **20**.

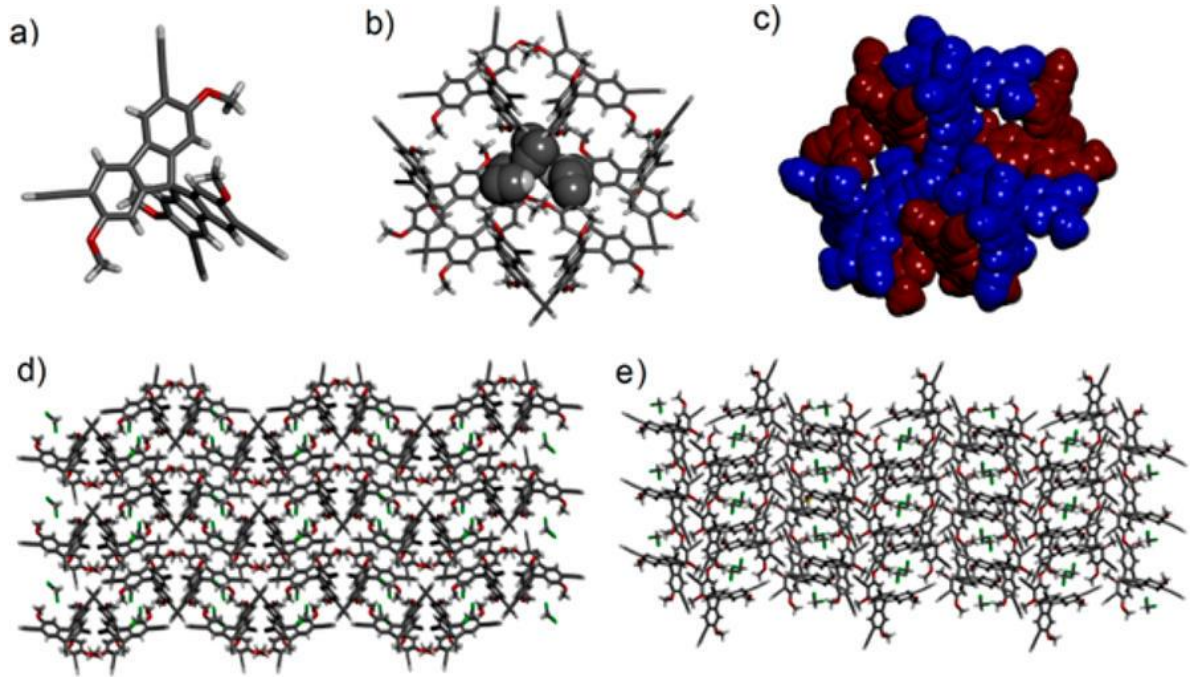

Figure 9. Crystal structure of **5:** (a) and of the associated hexamers $\mathbf{5}_6$ in stick (b) and CPK (c) representations; top (d) and side view (e) of the crystal packing of **5**.

What is really interesting about these structures is the fact that none of the classical directional interactions (*i.e*. electrostatic forces or hydrogen bonding) are not involved in the self-assembly process. The peripheral aromatic rings have van

der Walls contact one to each other, many of them being strongly connected in the self-assembled aggregates.[19,20,21]

An important structural detail refers to dipolar interactions between the electron-donor CH_3O-groups and the grafted electron-acceptor -I, -C≡N, -NO_2, and -C≡CH groups. In particular, we discovered that the donating CH_3O dipolar groups surround circular cavities pointing out from the cavities, while the acceptor dipolar groups (-I, -C≡N, and -C≡CH) are oriented toward the centre of the supramolecular hexameric or tetrameric structures. The supramolecular arrangement depends on the geometry, nature and spatial orientation of the interacting dipolar groups: two oppositely oriented dipoles for -C≡N groups, three iodine atoms, and six acetylene groups leading to hexamer structures. This may clearly explain the solid-state packing and the relative spatial orientation of the 9,9'-spirobifluorene.

The 9,9′-spirobifluorenes **3**, **20** and **5** are organized in crystal so that each successive molecule has an alternate chirality. Moreover, overall the crystal is racemic: homochiral monomers of opposite chirality are stratified.

The specific central packing observed for -I, -C≡N, -C≡CH groups, which are packed in the central part of the structure in symmetrical arrangements, could not be observed in the case of compound **23**, most probably because of the electronic nature and geometrical behaviour of the -NO_2 group.

Therefore, although the nitro- derivative **23** also forms hexameric aggregate the packing of this compound is different from that of the compounds with other substituents. Thus, in the crystal each spirobifluorene molecules of one chirality is interacting with six spirobifluorene molecules of the same chirality so that each molecule displays a tight contact (**Figure 7 b,e**). This results in the propagation of chiral information, with the formation of a homochiral crystal.[22]

Crystallization favours formation of networks that affords a closer molecular packing, thereby optimizing the hydrophobic interactions.

The hydrophobic packing no matter the tetrameric or hexameric motifs, imposes a different lamellar array in which the spirofluorene molecules run in two nearly perpendicular directions to generate the mesh interweaved layers.**(Figures 6-9 d,e)**

---

[19] Lions, F.; Martin, K. V. *J. Am. Chem. Soc*. **1957**, *79*, 2733-2738.
[20] Legrand, Y. M.; Dumitru, F.; van der Lee, A.; Barboiu, M. *Supramol. Chem*. **2009**, *21*, 230-237.
[21] Morimoto, T.; Uno, H.; Furuta, H. *Angew. Chem. Int. Ed*. **2007**, *46*, 3672-3675.
[22](a) Dumitru, F.; Petit, E.; van der Lee, A.; Barboiu, M. *Eur. J. Inorg. Chem*. **2005**, 4255-4262. (b) Dumitru, F.; Legrand, Y. M.; van der Lee, A.; Barboiu, M*. Chem. Commun.***2009**, 2667-2669.

II.5 Conclusion

A new efficient strategy for the synthesis of 3,3',6.6'-tetrasubstituted-9,9'-spirobifluorene derivatives with tetrahedral orientation of the substituents has been developed starting from 2,2',7,7'-tetraiodo-9,9'–spirobifluorene. The strategy involves in the first step the introduction of the methoxy functional group by an aromatic nucleophilic substitution reaction. Next, the 2,2',7,7'-tetrametoxy-9,9'–spirobifluorene derivative was submitted to a series of electrophilic substitution and coupling reaction, that resulted in the synthesis of 10 new functionalized compounds with different terminal groups $–OCH_3$, -I, ethynyl, 4-Py, -CN, -CHO, $-NH_2$,-COOH, $-NO_2$ in the required positions.

The structures of the compounds were determined by NMR (^1H, ^{13}C) HRMS, FT-IR , UV–Vis and, in the case of four derivatives, by X-ray diffraction. The molecular single crystals of these compounds are very similar. However, their unit cell associations are highly dependent on the nature of the substituents and led to the formation of triangular hexamers, extended hexamers, square tetramers and star shaped hexamers. Interestingly, in spite of the presence of polar groups in the structure of these compounds, the associations are exclusively formed by hydrophobic interactions. Moreover, crystallization favoured formation of networks that permit closer molecular packing, optimizing the hydrophobic interactions.

Chapter III. New Nucleobases Decorated Tetragonal and Tetrahedral Ligands

III.1 Introduction

The continuous development in the construction of porous materials with specific applications, through self-assembly by supramolecular interactions, has prompted us to combine the structure particularities of some tetrahedral or tetragonal based ligands with the nucleobases abilities to form hydrogen bonding.

In this chapter we present the CuAAC (Copper-catalyzed Azide-Alkyne Cycloaddition) mediated-synthesis and characterization of new, rigid nucleobases-

decorated tetrapodands exhibiting 1,3,5,7-tetraphenyladamantane and 9,9′-spirobifluorene central units.[23]

Derivatives of tetraphenyladamantane and 9,9'-spirobifluorene are interesting building blocks that can be used for the construction of 2D and 3D molecular architectures.

Structural characterization of the reaction products was carried out by Nuclear Magnetic Resonance Spectroscopy (1D: ^{1}H-NMR, ^{13}C-NMR and 2D-COSY) and high resolution mass spectrometry (HRMS).

III.3 Objective

Our goal was the synthesis and structural characterization of new nucleobases-decorated tetrapodands for hydrogen-bonding directed construction of organic frameworks.

The target ligands **I, II** and **III** contain a tetrahedral **(I, III)** and tetragonal **(II)** core conjugated to different nucleobases through a rigid linker**.** (**Figure 10**)

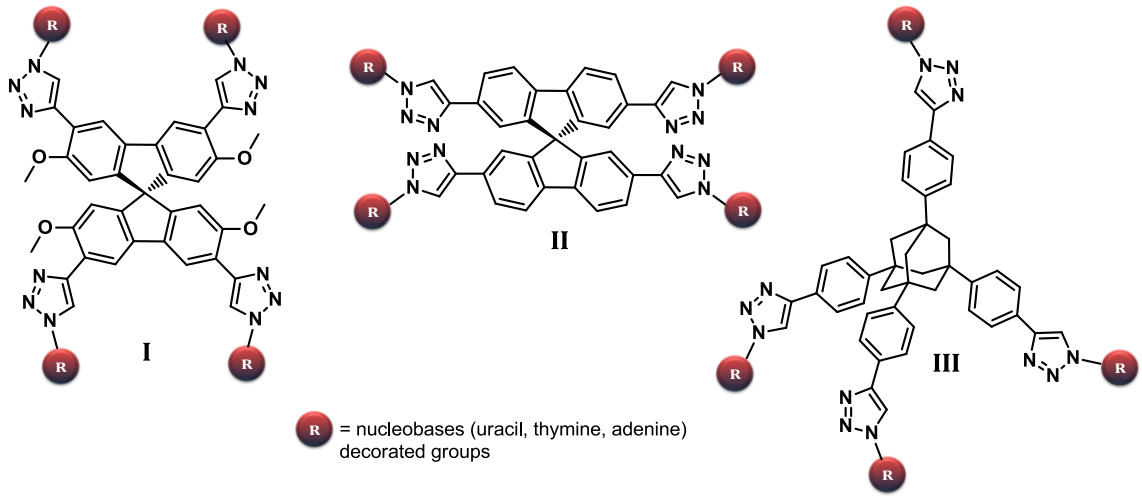

Figure 10. General structure of the target nucleobases-decorated tetrasubstituted adamantane **III** and 9, 9′-spirobifluorene **I**, **II** building blocks

[23]Pop, L.; Golban, M. L.; Hădade, N. D.; Socaci, C.; Grosu, I**.** *Synthesis* **2015,** *47*, 2799-2804.

III.4 Results and discussions

III.4.1 Synthesis of the ligands

In order to obtain our target structures, the adamantane and spirobifluorene derivatives with tetrahedral and tetragonal geometry, bearing appropriate reactive groups at the required positions, were synthesized (**Figure 11**).

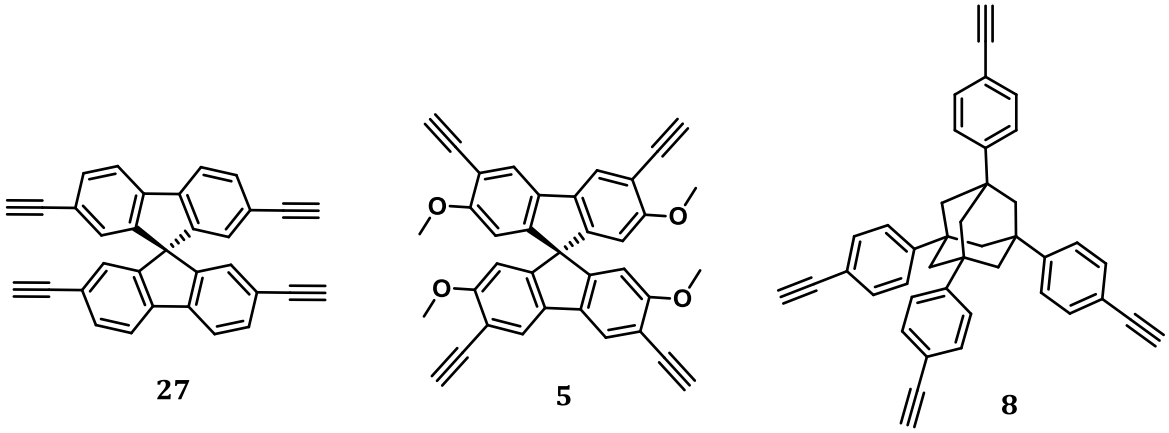

Figure 11. Tetrapodal ligands used in „*click*" reactions with azide-functionalized nucleobases

The synthesis of tetrapodand **27** was carried out according to a previously described procedure, starting from the corresponding tetraiodo-9,9'-spirobifluorene derivative **1** (**Scheme 1**, **Chapter I**)

Scheme 19. Synthetic Scheme for Preparation of Compound **27** from Compound **1**

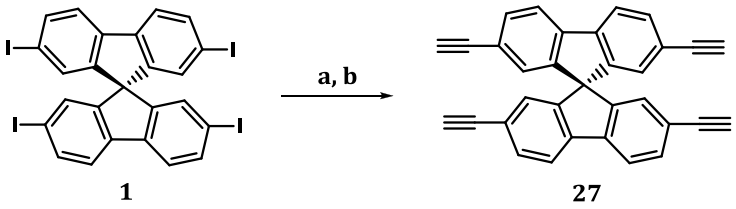

Reagents and conditions*: a.* TMS-acetylene, Et_3N, $(Ph_3P)_2PdCl_2$, CuI, C_6H_5-CH_3;**b:** KF, CH_3OH

The tetraethynyl derivative **5** (see **Scheme 4**, **Chapter I**) was required for the preparation the target compound **36.** Therefore, we firstly synthesised the tetraiodinated derivative **1** (I_2, PIFA, $CHCl_3$) in good yields, starting from spirobifluorene **I**

Compound **8** was obtained in a four steps synthesis using a previously described method[24]: Friedel-Crafts reaction between bromo-adamantane and benzene, followed by the iodination of the tetraphenyladamantane, Sonogashira cross coupling and finally the deprotection of the TMS groups. (see also **Schemes 5,6** in **Chapter I**)

Nucleobases **28**, **29**, **30** (**Figure 12**) functionalized with azide groups and exhibiting the *p*-xylylene unit as spacer were obtained using a procedure recently developed in our group.[25]

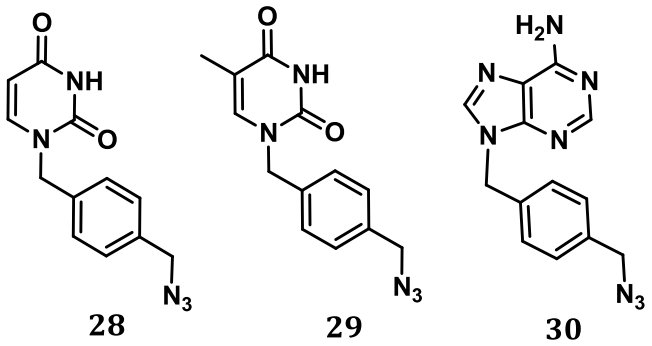

Figure 12. Uracil (**28**), thymine (**29**) and adenine (**30**) functionalized derivatives

III.4.2 Synthesis and structural analysis of the target nucleobases-decorated ligands

The synthesis of the target nucleobases (uracil, thymine, and adenine) -decorated tetrapodands were performed in very good yields by copper-catalyzed azide-alkyne cycloadditions (CuAAC; ,,click'' reaction; **Schemes 20–22**) using tetragonal and the tetrahedral tetraalkynes **5**, **8** and **27**, and the azide-decorated nucleobases **28, 29, 30**.

Taking advantage of the same *click* reaction, compounds **31**, **32**, **33** (**Scheme 20**) were obtained by the reactions between of tetrapodand **8** and three azides functionalized nucleobases (uracil, thymine and adenine) under classic reaction conditions. Thus, THF was used as solvent at room temperature, for 12 hours. The Cu(I) catalyst was generated *in situ* from $CuSO_4x5H_2O$ using TBTA

[24] (a) V. R. Reichert, V. R.; Mathias, L. J. *Macromolecules,* **1994**, *27*, 7015-7023.
[25] Golban, M. L.; Paşcanu, V.; Hădade, N. D.; Pop, L.; Socaci, C.; Grosu, I. *Synthesis,* **2014**, *46*, 1229-1235.

[Tris(benzyltriazolylmethyl)amine] as ligand in presence of sodium ascorbate as reducing agent. All compounds were obtained as white solids that precipitated from the reaction mixtures, washed with *N*-(hydroxyethyl)ethylenediaminetriacetic acid (HEDTA) (3 × 20 mL), MeOH (3×20 mL), and did not required further purifications. The reactions were monitored by TLC and full conversion of **8** was observed in all cases.

Scheme 20. Synthetic Scheme for Preparation of Compounds **31, 32** and **33** from Compound **8**

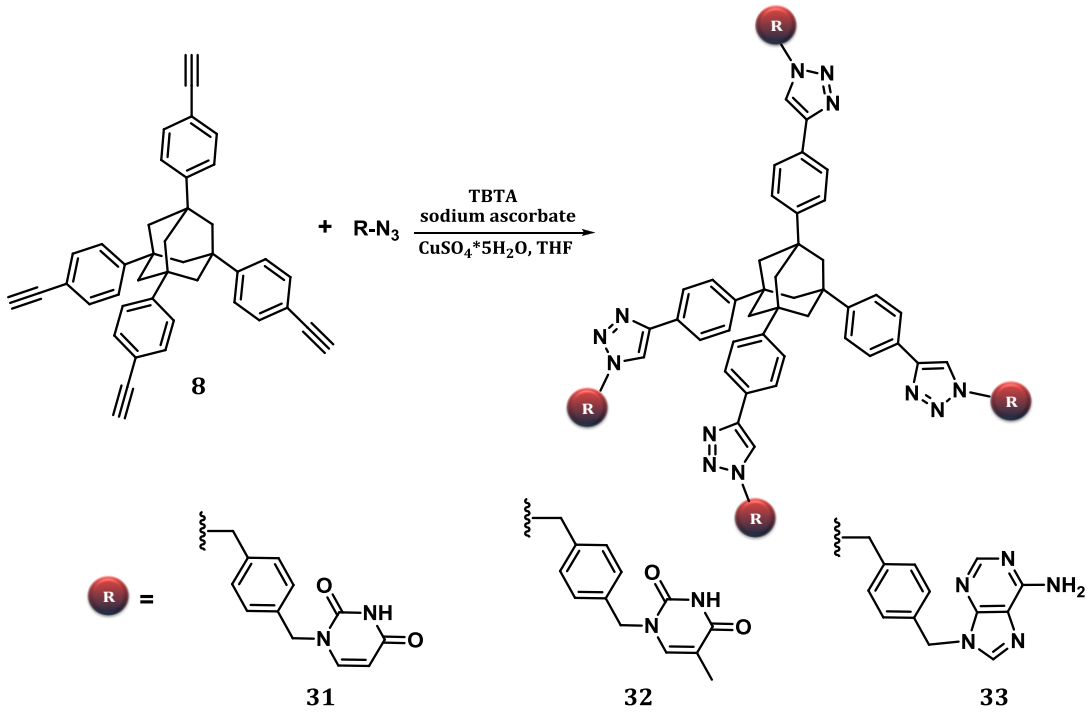

All structures were confirmed by NMR and HRMS analysis. For example the ^{1}HNMR spectrum of ligand **32** presents the expected signals for the thymine, tetraphenyladamantane and linker units which are shown in **Figure 13** in red, blue and purple respectively.

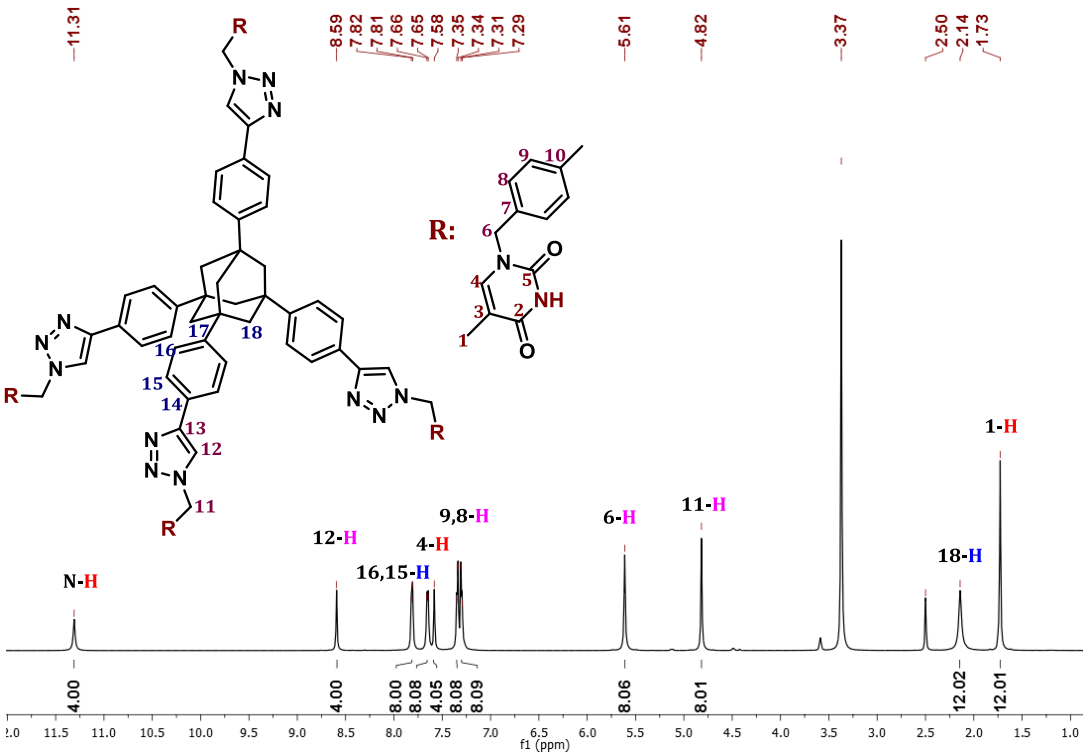

Figure 13.^{1}H NMR [$(CD_3)_2SO$, 600 MHz] spectrum of compound **32**

The key step in the synthesis of compounds **34** and **35** was also the CuAAC- *click chemistry* reaction between the alkyne decorated tetragonal ligand **27** and the azide functionalized nucleobases, **28** and **29.**

Scheme 21.Synthetic Scheme for Preparation of Compounds **34** and **35** from Compound **27**

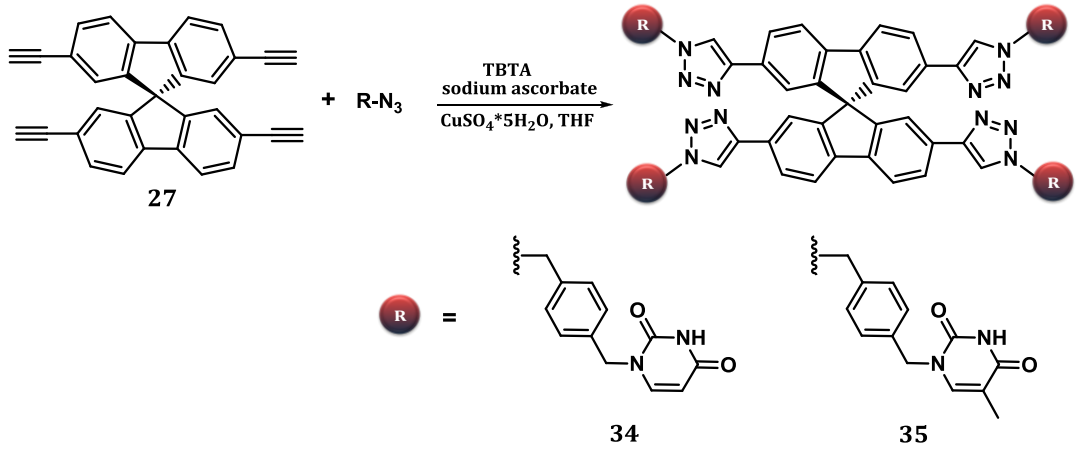

The click chemistry reaction was performed in THF as solvent using $CuSO_4x5H_2O$ as copper source, TBTA as metal coordinating ligand and sodium ascorbate as reducing agent. Stirring at room temperature for 12h furnished the target compounds

34 and **35** which were isolated in pure form in very good yields (86 and 91 % respectively).

Confirmation of the structural identity for compound **34** was performed by ^{1}H NMR and 2D- COSY.

Compound **36** (**Scheme 22**) was obtained in similar conditions as the ones described above through a click chemistry reaction. Compound **36** was obtained as yellow solid in very good yield (92%) and was fully characterized by NMR spectroscopy (^{1}H, ^{13}C) and high resolution mass spectrometry (HRMS).

Scheme 22. Synthetic Scheme for Preparation of Compound **36** from Compound **5**

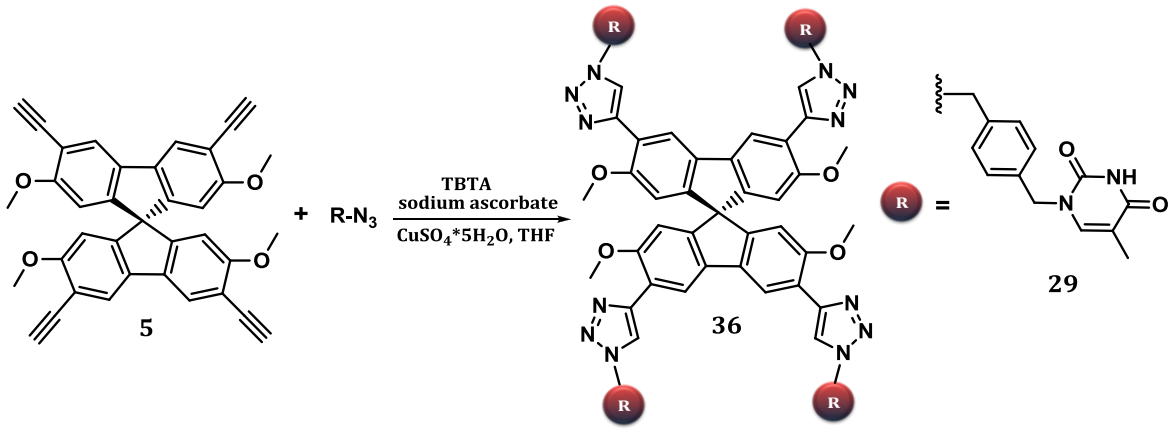

III.5 Conclusions

Four new nucleobases (uracil, adenine, thymine)-decorated ligands with tetrahedral structure were obtained starting from tetraphenyladamantane or 3,3',6,6'–tetrasubstituted-9,9'-spirobifluorene derivatives bearing ethynyl terminal groups (**31**, **32**, **33**, **36**) and azide decorated nuclebases. The ligands with tetragonal structure (**34**, **35**) were obtained starting from 2,2',7,7'-tetrasubstituted 9,9'-spirobifluorene derivatives.

The target nucleobases-decorated tetrapodands were obtained using CuAAC ,,click" reaction in high yields.

The newly synthesized ligands display all the necessary structural characteristics of building blocks usually encountered in 2D or 3D organic frameworks. These compounds will be further used for the construction of self-assembled networks, either through hydrogen bonding or by metal-ion induced associations.

The structure of compounds **31-36** was confirmed by NMR spectroscopy (1D, 2D) and High Resolution Mass Spectrometry (HRMS)

Chapter IV. Metal Organic Frameworks (MOFs) based on tetrahedral and tetragonal ligands

IV.1 Introduction

Bearing in mind the recent advancement in the field of MOFs and their fascinating applications, our goal was to design and synthesize ligands with tetrahedral and tetragonal geometry (**Figure 14**) that can be used as building blocks for the construction of new MOFs with improved properties. Therefore, we turned our sights toward tetraphenyladamantane derivatives, having tetrahedral geometry, to build 3D MOFs and 2,2',7,7'-tetrasubstituted-9,9'-spirobifluorenes, with tetragonal geometry, to obtain 2D MOFs (**Figure 14**).

The synthesis of target compounds, having in their structure functional groups able to act as complexation site for various metal-ions such as Cu^{+2}, Fe^{+2} was imagined using different types of reactions (*i.e.* substitution reaction, Suzuki coupling reaction, etc.)

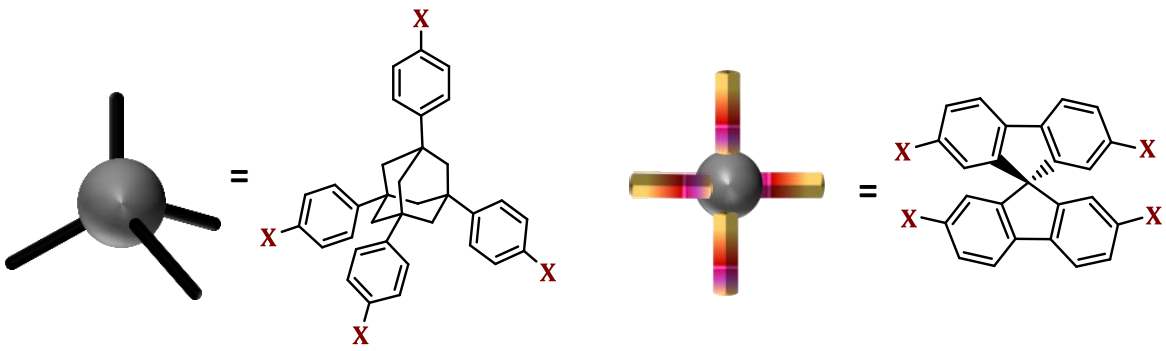

Figure 14. Structure of tetraphenyladamantane and 9, 9' spirobifluorene based ligands

Synthesis and characterization of the ligands was performed at Babes-Bolyai University while the complexation reactions, the crystallization and characterization of new MOFs were carried out in collaboration with the Theoretical Inorganic and

Applied Chemistry Research Group, coordinated by Acad. Prof. Marius Andruh, at University of Bucharest.

IV.3.1. 9, 9' Spirobifluorene based ligands

Among the different ligands with tetragonal structures that could be used for the obtaining of 2D-MOFs we stopped to 9,9'-spirobifluorene derivatives decorated with different functional groups *(i.e.* -COOH, -CN, -4-Py*)* at positions 2,2',7,7'. The synthesis of all these derivatives have as starting point the 9,9'-spirobifluorene central motif **I** (see **Scheme 1**, **Chapter I**).

Compound **37** (**Scheme 23**) was obtained from tetraiodo derivative **1** (see **Scheme 1**, **Chapter I**) using the classical Rosenmund-von Braun reaction under conditions previously described in the literature.[26]

Scheme 23. Synthetic Scheme for Preparation of Compound **37** from Compound **1**

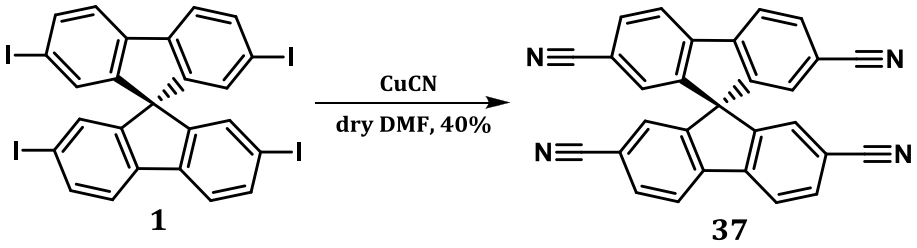

1 **37**

Next, compound **38** was synthesized by hydrolysis of nitrile groups, performed under basic conditions. Thus, firstly **37** was refluxed with aqueous KOH solution in ethanol as solvent. Tetracarboxylic acid **38** was obtained after its release from the potassium carboxylate by acidification with hydrochloric acid. **(Scheme 24)**

[26] Holy, P.; Havlik, M.; Tichy, M.; Zavada, J.; Cisarova, I. . *Collect. Czech. Chem. Commun*. **2006**, *71*, 139-154.

Scheme 24. Synthetic Scheme for Preparation of Compound **38** from Compound **37**

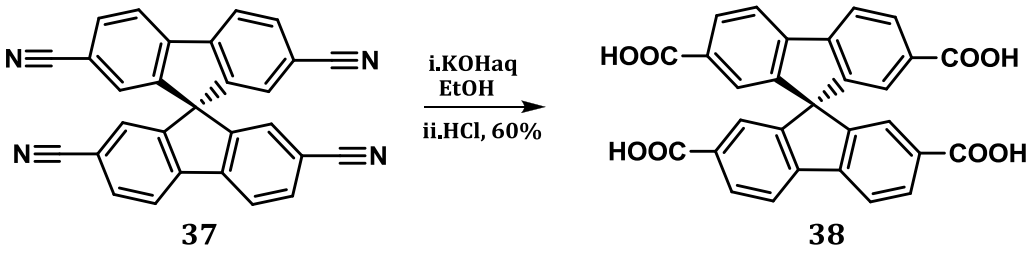

37 **38**

2,2′,7,7′-Tetra(pyrid-4-yl)-9,9′-spirobifluorene, compound **39 (Scheme 25)**, was obtained following a modified literature procedure[27] by Suzuki coupling of 4-pyridinylboronic acid with spirobifluorene derivative **1** (**Scheme 1**, **Chapter I**) in presence of Na_2CO_3 as base and [1,1′ Bis(diphenylphosphino)ferrocene] dichloropalladium(II) as catalyst using a dioxane/water mixture as solvent and under Ar atmosphere.

Scheme 25. Synthetic Scheme for Preparation of Compound **39** from Compound **1**

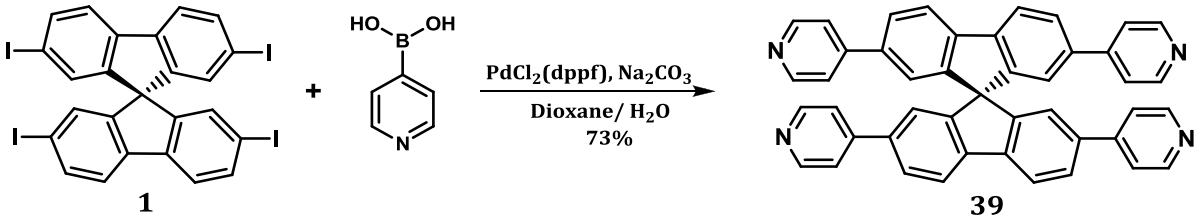

1 **39**

IV.3.2. Tetraphenyladamantane based ligands

Tetrasubstituted-tetraphenyladamantane derivatives with tetrahedral orientation, decorated with different reactive groups (4-Py, -CN, -CHO, -tpy -COOH,) were synthesized starting from 1,3,5,7 tetraphenyladamantane. These compounds were investigated as building blocks for the construction of metal-organic frameworks (MOFs).

Compound **40** was obtained according to the literature data,[28] through the reaction of **II** (for the synthesis of II see **Scheme 5**, **Chapter I**) with excess of

[27] Li, X.; Zhang, J.; Zhao, Y.; Zhao, X.; Li, F.; Li, T.; Li, H. L.; Liang, Chen. *J. Mater. Chem. A*, **2015**, *3*, 6265-6270.

[28] Duncan, N. C.; Hay, B. P.; Hagaman, E. W.; Custelcean, R. *Tetrahedron*, **2012**, *68*, 53-64.

dichloromethyl methyl ether, at 0^0C, in presence of titanium tetrachloride as catalyst and anhydrous DCM as solvent, under inert atmosphere (Ar).

Scheme 26 Synthetic Scheme for Preparation of Compound **40** from Compound **II**

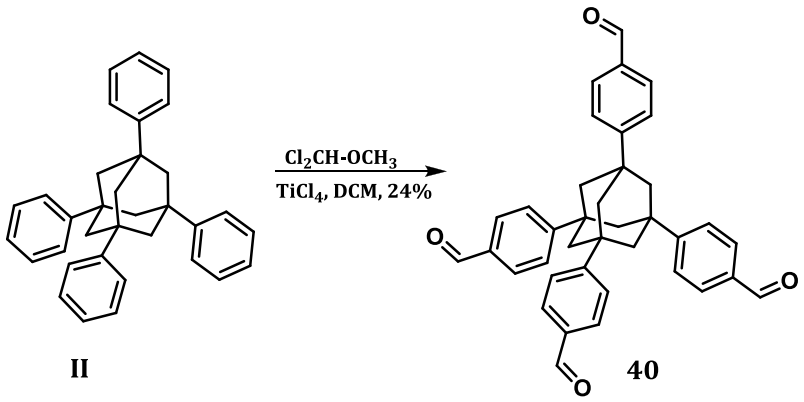

Starting from derivative **40** by a classical oxidation reaction[29], we obtained compound **41** (**Scheme 27**). The oxidation reaction was carried out with NaClO at 0°C, in the presence of $NiCl_2$ hexahydrate, in a mixture of DCM/H_2O. The reaction mixture was stirred for 4 hours. Finally the compound was isolated as a white powder, in 45% yield.

Scheme 27. Synthetic Scheme for Preparation of Compound **41** from Compound **40**

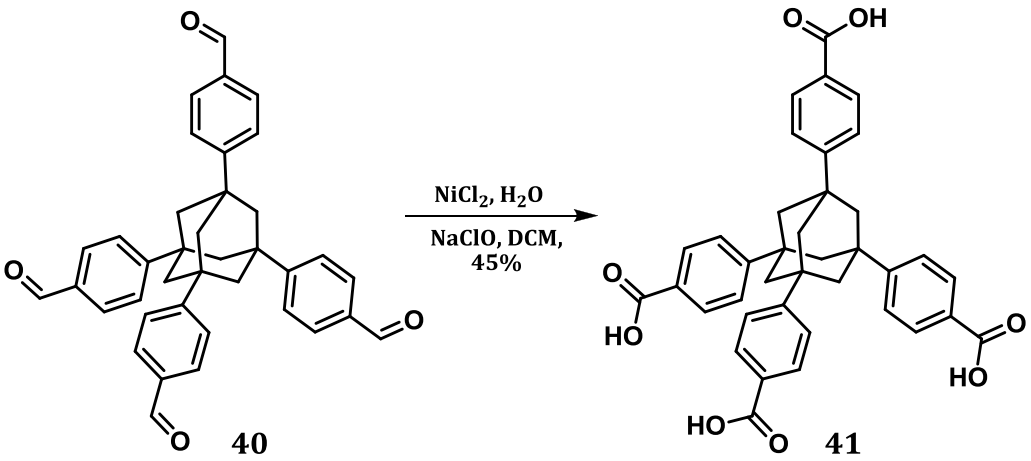

Finally, the tetracyanoderivative **42** was obtained by a substitution reaction. The aromatic nitriles groups can act as binding sites for various metals and, also, can be easily transformed into different functional groups (-R-COO-R, -$RCONH_2$, -R-

[29] Grill, J. M.; Ogle, J. W.; Miller, S. A. *J. Org. Chem*. **2006**, *71*, 9291-9296.

COOH). The ligand **42** (**Scheme 28**) was obtained, according to the literature data.[30] The reaction was performed in anhydrous DMF, under inert atmosphere, and the copper cyanide was added in excess. (1.1 eq./group)

Scheme 28. Synthetic Scheme for Preparation of Compound **42** from Compound **6**

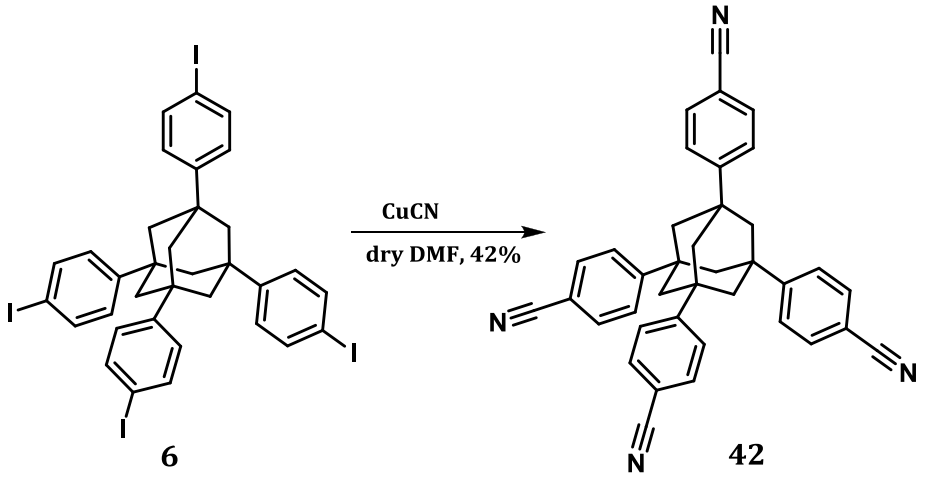

6 **42**

In order to obtain the compound **43** we used Suzuki-Miyaura coupling reaction, carried out under palladium(0) catalysis. The reaction was performed using the intermediate **6** (see also **Scheme 6**, **Chapter I**) and 4-pyridinylboronic acid in the presence of $Pd(dppf)Cl_2$, under inert atmosphere (in order to prevent air oxidation of the sensitive catalyst) and Na_2CO_3 as a base. As solvent we used a mixture of dioxane/water, and the optimal temperature was 80°C. For the purification of the crude product we used column chromatography .The desired compound was obtained as a white solid, in good yield (40%). (**Scheme 29**)

[30] Boldog, I.; Domasevitch, K. V.; Baburin, I. A.; Ott, H.; Gil-Hernández, B.; Sanchiz, J.; Janiak, C. *CrystEngComm***. 2013**, ***15***, 1235-1243.

Scheme 29. Synthetic Scheme for Preparation of Compound **43** from Compound **6**

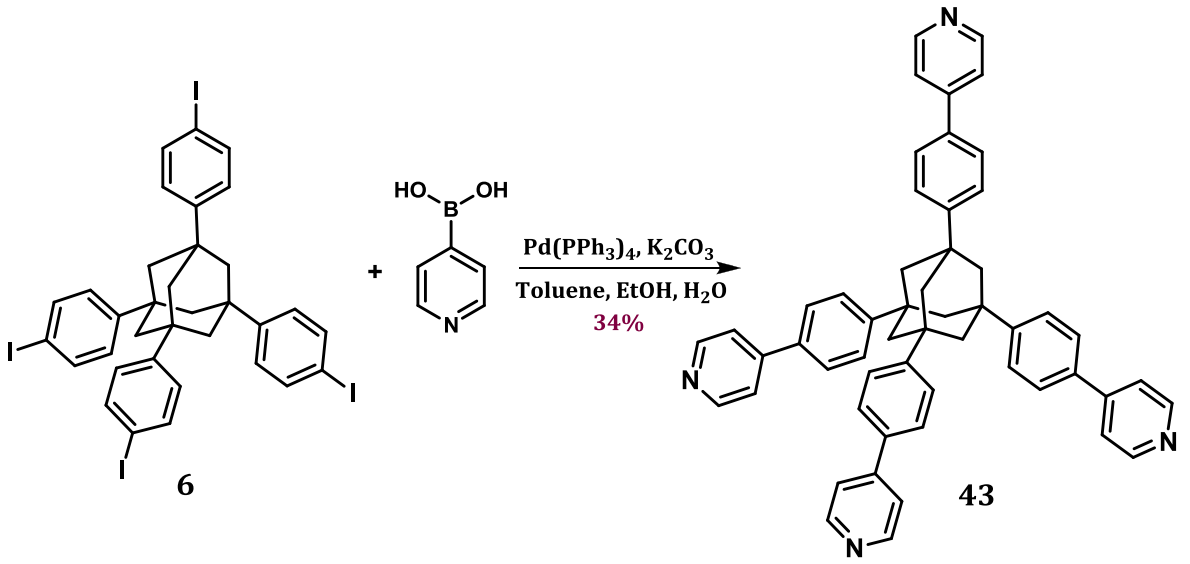

In the last decades, compounds decorated with terpyridine units have been the subject of many publications. The major interest for the synthesis of these derivatives is given by the affinity of terpyridine motif for various metal-ions (*i.e.* mainly transitional metal-ions) and their utility in the obtaining of various metal-ion directed supramolecular assemblies. Based on terpyridine complexation capacity with different of metals ions (*i.e.* Fe(II), Ni(II), Zn(II), Cu(II) etc.) these compounds are presented as main ligands in the coordination chemistry. [31,32]

In order to obtain the ligand **46** that contains four terpyridine units, we synthesized first the intermediate **45** (**Scheme 30**) in two steps, following a procedures described in the literature. The starting materials used to obtain 4'-(4-bromophenyl)-2,2':6',2''-terpyridine (**44**) were the 4-bromobenzaldehyde and 2-acetylpyridine, the reaction occurred at reflux in basic conditions. The next step was the transformation of derivative **44** in the boronic ester derivative **45**.

[31] Cooke, M. W.; Hanan, G. S. *Chem. Soc. Rev.* **2007**, *36*, 1466-1476.
[32] Constable, E. C. *Chem. Soc. Rev.* **2007**, *36*, 246-253.

Scheme 30. Synthetic Scheme for Preparation of Compound **45** from Compound **44**

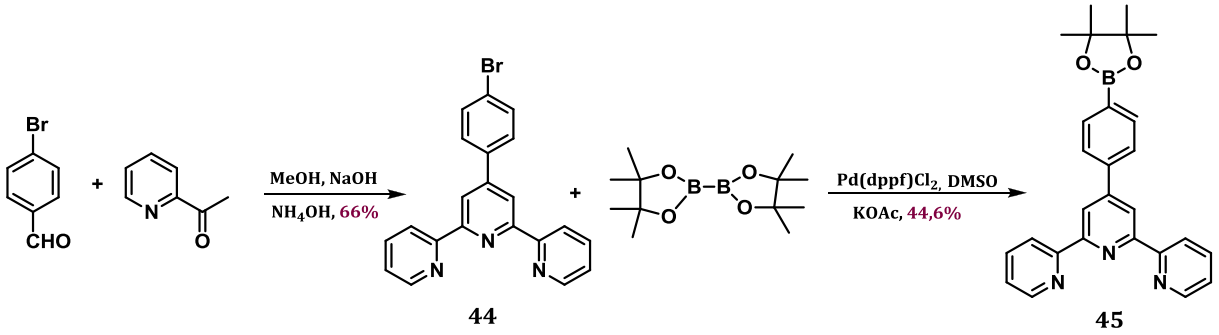

Intermolecular Suzuki coupling reaction of boronic ester **45** and the tetraiodo derivative **6** has resulted in tetra terpyridine functionalized ligand **46.** (**Scheme 31**)

Scheme 31. Synthetic Scheme for Preparation of Compound **46** from Compound **6**

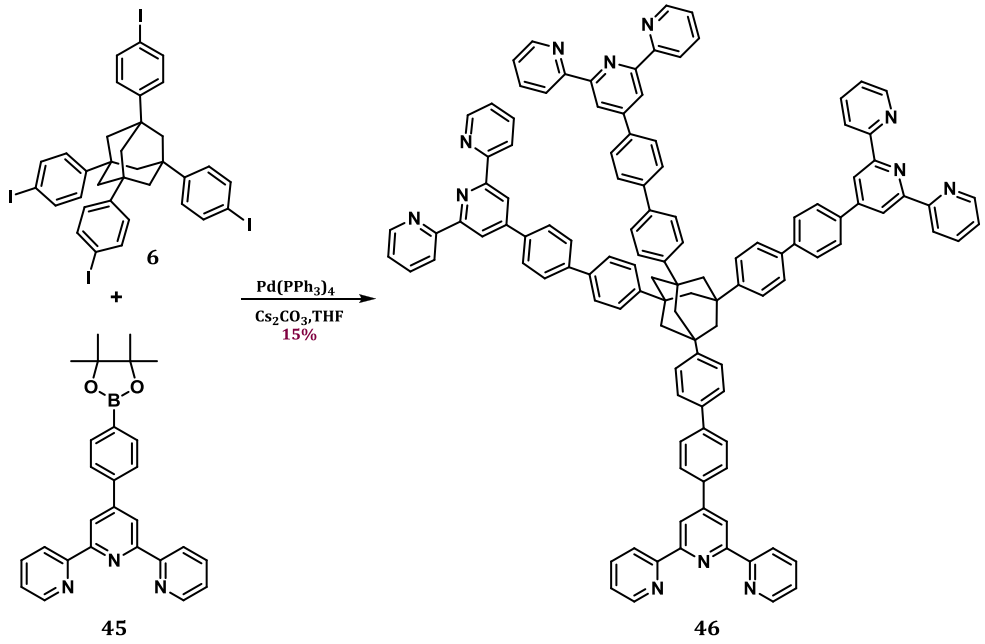

The synthesis involved classic reaction conditions for the Suzuki coupling using $Pd(PPh_3)_4$ catalyst (8% mol), Cs_2CO_3 as base in THF at reflux for 48 hours. The removal of the reaction by products was carried out by repeated washings with EtOH and diethyl ether. The pure ligand was obtained as a beige powder in 15 % yield. The pure ligand **46** was characterized by ^{1}H NMR, ^{13}C NMR and by ESI(+)-HRMS.

Metal complexes

Ligand **46** was further used in several complexation reactions. Thus, treatment of **46** with Fe(II) (using iron perchlorate pentahydrate as iron(II) source) resulted in the Fe(II)-**46** complex as a purple, insoluble product. Unfortunate, because of its high insolubility, we were not able to obtain single crystals suitable for X-ray analysis.

Complexation of **46** with Cu(II) (Copper(II) acetate monohydrate) and Zn(II) (zinc acetate dyhidrate) in presence of 5 5'-dimethyl-2 2'-bipyridine (in a molar ratio **46** / M(II) / 5,5'-dimethyl-2 2'-bipyridine = 1/4/4) in various solvent mixture (*i.e.* THF/H_2O, AcCN/H_2O) yielded mixed complexes that were analyzed by mass spectrometry(ES-MS).

IV.3.3 MOFs based on tetraphenyladamantane tetrahedral motifs

Metal-ion induced self-assembly of organic ligands is an important process in the field of supramolecular chemistry. Numerous examples of self-assembled metal complexes that resulted in architectures with well defines structures and shapes (*i.e.* shelves, stairs, cages etc.) were reported in the literature. Moreover, as shown in the introduction part, 2D and 3D MOFs obtained from various organic ligands and metal ions, were investigated both from structural point of view and their potential applications.

Two ligands **42**, **43**, (see **Schemes 28** and **29**, **Chapter IV**) with tetrahedral structure that contains metal coordinating sites were used in metal-ion induced self-assembly processes to obtain 3D metal-organic networks. The structure of the organic-inorganic networks was characterized by single-crystal X-ray diffraction.

Complexation of the ligand 1, 3, 5, 7-tetrakis (4-cyanophenyl) adamantane (**42**) with manganese (II) hexafluoroacetylacetonate led to a 3D that was investigated using single crystal X-ray determinations.

Figure 15 shows a representation of the obtained network. It contains series of tetrahedral units (the ligand **42**) connected by angular junctions, provided by the Mn(II) metal-ion. Mn(II) has the coordination number six. Mn(II) forms equatorial and axial coordination bonds with ligand **42** as well as equatorial-axial and equatorial - equatorial coordination bonds with two hexafluoroacetylacetonate ligands (**Figure 15**).

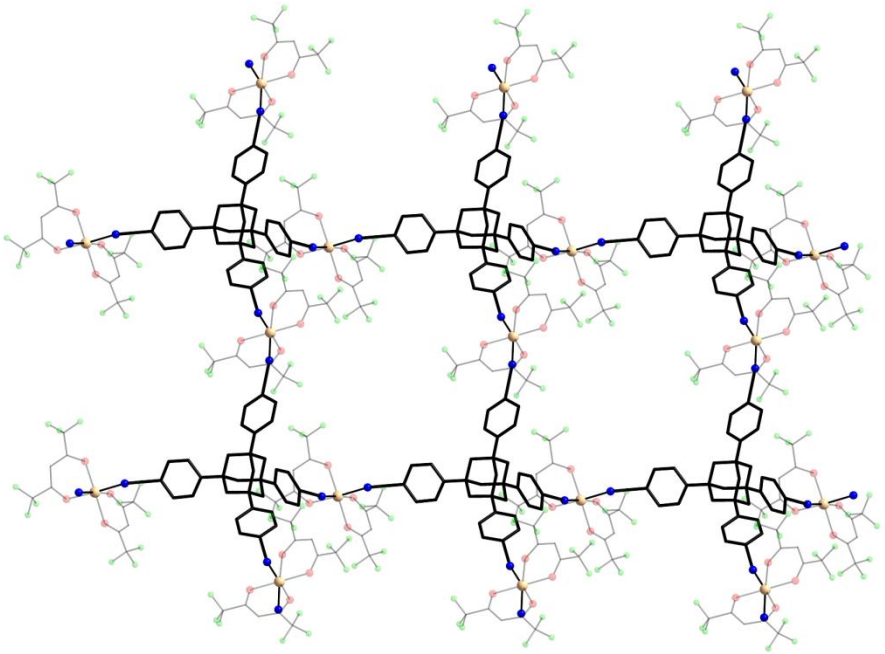

Figure 15. Representation of the 3D network obtained from **42** in presence of Mn(II) and hexafluoroacetylacetonate co-ligand

Another interesting metal organic network was obtained by complexation of compound **43** with copper (II) metal ions. Single crystal X-ray 3D molecular structure of the complex (**Figure 16**) has a PtS topology. The network contains two types of nodes: with tetrahedral geometry (the 1,3,5,7 - tetrakis {4- (4-pyridyl) phenyl} adamantane ligand **43**, represented in yellow) and squares planar geometry (Copper(II) ions, represented in dark green) respectively. For clarity, for the copper nodes, only the bonds leading to expansion the network in the three dimensions are represented. (**Figure 16**).

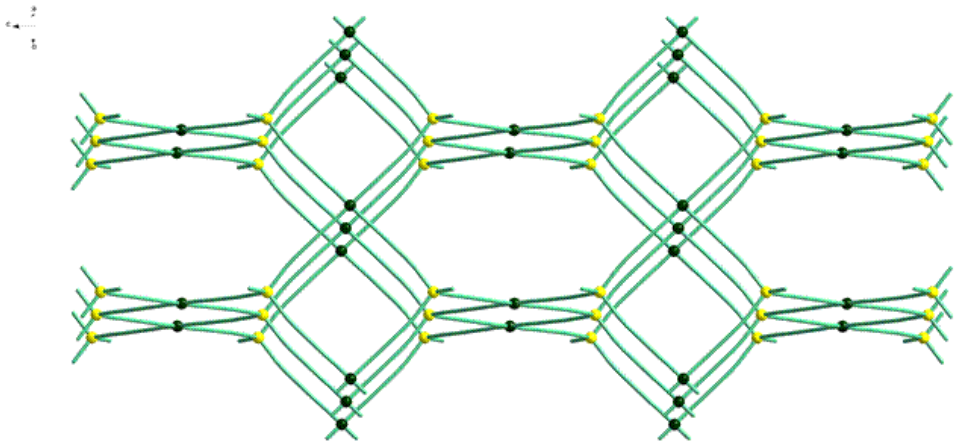

Figure 16. Representation of the 3D network obtained from **43** in presence of Cu (II)

The lattice of the complex **43-**Cu(II) (**Figure 17**) contains four interpenetrating networks represented in red, grey, green and pink, respectively.

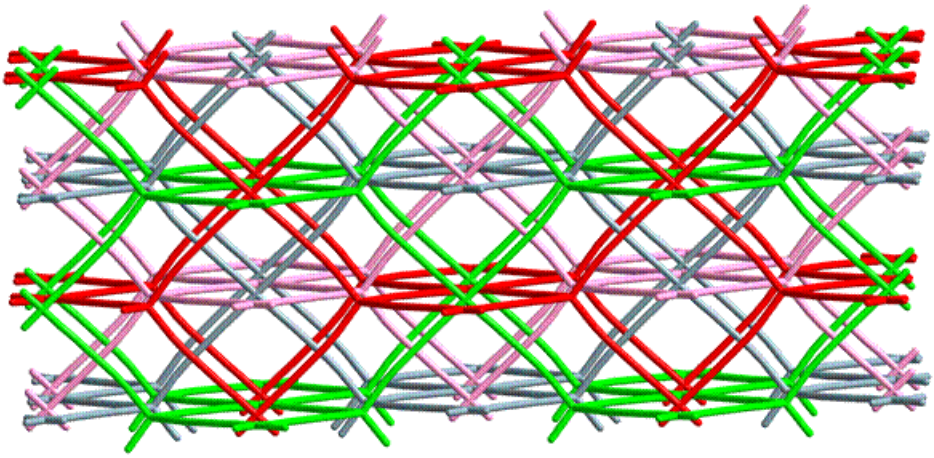

Figure 17. Representation of the lattice of **43-**Cu(II) network showing four 3D interpenetrating network

Finally, complexation of the ligand **43** with Cu(I) yielded a 3D network, formed by of 1,3,5,7-tetrakis {4- (4-pyridyl) phenyl} adamantane units (represented in gray), with tetrahedral geometry, and Cu(I) nodes (represented in blue), with square planar coordination geometry.

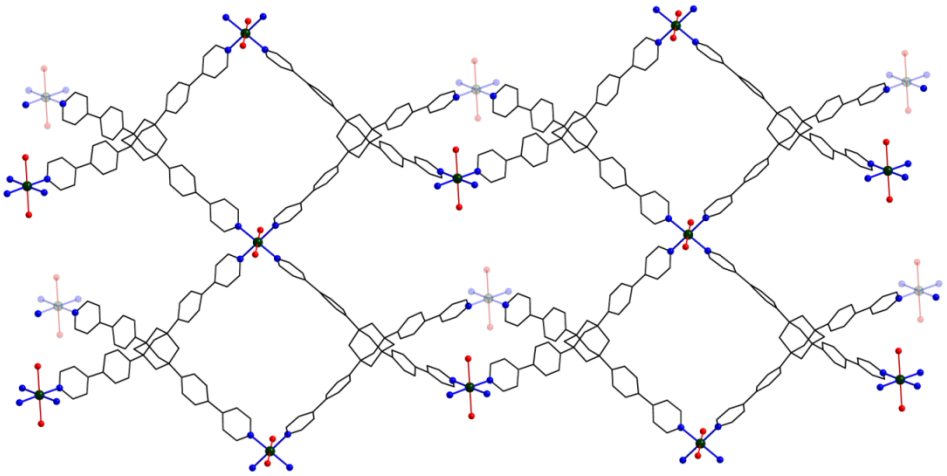

Figure 18. Representation of the 3D network obtained from **43** in presence of Cu(I)

IV.4 Conclusions

In conclusion, we obtained ligands with tetragonal and tetrahedral geometry that contain the 9,9'-spirobifluorene or tetraphenyladamantane motifs, respectively. These ligands were decorated with various functional groups (*i.e.* -CN, -Py, -TPy, -COOH, -CHO) and their structure was analyzed by mass spectrometry and NMR spectroscopy. All these ligands have metal coordination site that can be exploit for the obtaining of new 2D and 3D MOFs.

In addition, a tetra-terpyridine functionalized ligand **46**, designed to serve as building block for the metal-ions induced construction of organic-inorganic frameworks, was obtained using the Suzuki cross-coupling reaction as key step of the synthetic strategy. Complexation of **46** with Fe(II) yielded a metal-organic network, while co-complexation of **46** and a bipyridine derivative with Zn(II), Fe(II) or Cu(II) metal-ions resulted in mixed complexes that were characterized by ESI(+)-HRMS.

Ligands **42** and **43** were successfully used in the obtaining of metal-organic frameworks with Mn(II), Cu(I) and Cu(II) metal-ions, respectively. The resulted MOFs were obtained as single crystal and characterized by X-ray diffraction.

Chapter V. Charge-Assisted Hydrogen Bonding Self-Assembly of bis-amidine complexes

V.1 Introduction

Bearing in mind the importance of non-covalent interactions for the construction of many interesting supramolecular architectures reported in the literature, we considered of interest to extend these studies for diamidine and dicarboxylate derivatives that can interact through a Charge-Assisted Hydrogen Bonding (CAHB) process. CAHB arises from the combination of two well-known interactions, namely electrostatic forces and H-bonding. (**Figure 19**)

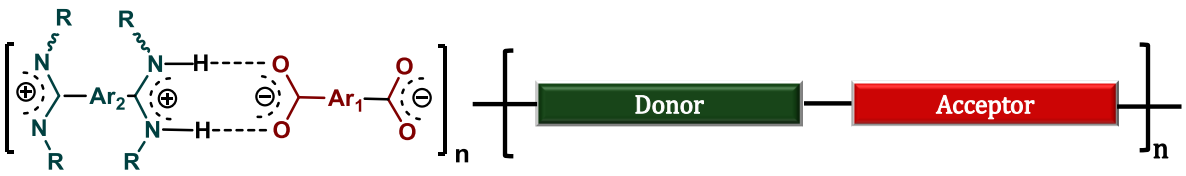

Figure 19. CAHB motif between the amidinium and the carboxylic acid moieties

CAHB amidinium-carboxylate associations can generate three diastereoisomers (***E***/***E***, ***E***/***Z*** and ***Z***/***Z***) that differ by the relative disposition of the substituents in the amidinium moiety. (**Figure 20**)

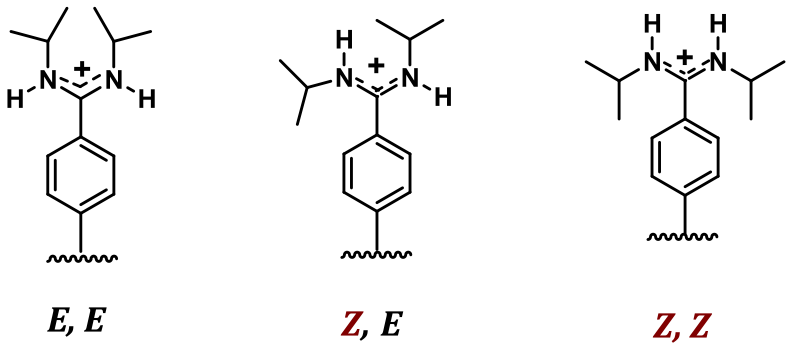

Figure 20. Representation of ***E-E***, ***E-Z*** and ***Z-Z*** diastereoisomers resulted by CAHB association of amidinium-carboxylate moieties

In this chapter we focused on the investigation of the CHAB supramolecular association of diamidinium dications **47** or **48** and the dianions of the dicarboxylic acids $\mathbf{A_1}$-$\mathbf{A_4}$ and the disulfonic acids $\mathbf{A_5}$, **A6** respectively. (**Figure 21**) We monitored the influence of the relative positions (*ortho*, *meta*, *para*-phenylene or 3,6-carbazole) of the carboxylate groups, in the case of $\mathbf{A_1}$-$\mathbf{A_4}$ and the sulfonic acid groups, 1,5 (in $\mathbf{A_5}$), 1,6 (in $\mathbf{A_6}$) on to the self-assembling process, as well as the effect of the sterical hindrance introduced by the bulky substituents (*N,N*-diisopropyl) in the amidine unit.

The supramolecular associations of these compounds were studied both in solution and in solid state and the results are described below.

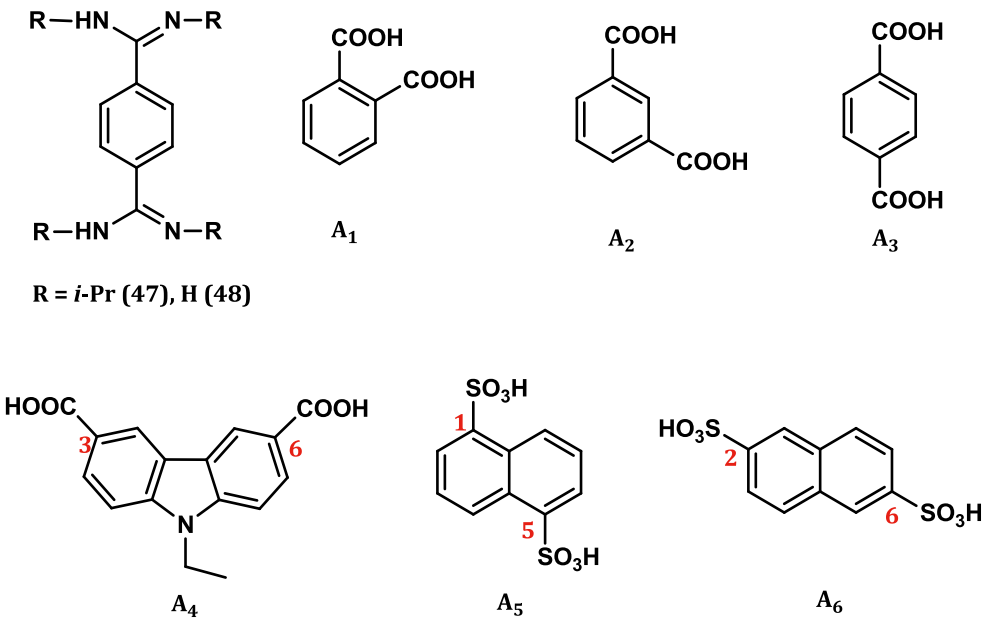

Figure 21. Chemical structure of the diamidines **47**, **48** and diacids **A_1-A_6** used in this study

V.3 Results and discussions

The supramolecular associations between various amidines and carboxylic or sulfonic acids were studied both in solution, by NMR spectroscopy (^{1}H, ^{13}C), and in solid state, through X-ray diffraction experiments.

V.3.1 Investigations in solution

Detailed solution investigations were performed using both amidines/ carboxylic or sulfonic acids and amidinium hydrochlorides/sodium carboxylates or sulfonates in methanol or aqueous solution, respectively.

For the experiments using salts as starting materials we used commercially available compounds, except in the case of compounds **47** and **A_4** that were synthesized using procedures previously reported in literature.[33,34,35]

[33] Grundy, J.; Coles, M. P.; Hitchcock, P. B. *J. Organomet. Chem*., **2002**, *662*, 178-187.
[34] *Zhou, H.; Zhou, F.; Tang, S.; Wu, P.; Chen, Y.; Tu, Y.; Wu, J.; Tian, Y. Dyes Pigm*, **2012**, *92*, 633-641.
[35] Holy, P.; Havlik, M.; Tichy, M.; Zavada, J.; Cisarova, I. *Collect.Czech. Chem. Commun*. **2006**, *71*, 139-154.

All supramolecular assemblies of type **xy** (x: **47**, **48**, y: **A_1-A_6** were obtained both in solid state and solution. Solid state synthesis consisted in vigorous grinding for 20 minutes of equimolecular amounts of diamines and diacids. The solids obtained after this process were taken in a small amount of water and the obtained solutions were used for crystallization and NMR investigations.

Solution synthesis involved the mixing of diamidine dihydrochlorides (**47**x**2HCl** or **48**x**2HCl**) with disodium salts of dicarboxylic acids **A_1**-**A_4** or disulfonic acids **A_5** and **A_6** using 1M aqueous solutions that were allowed to stand two days before crystallisation or preparation of the NMR samples. The ^{1}H NMR spectra of compounds **47A_{1-6}** and **48A_{1-6}** exhibit a significant modification of the chemical shifts for all signals as compared to the corresponding signals in the ^{1}H-NMR spectra of the isolated diamidines **47** or **47**x**HCl** and **48** or **48**x**HCl** respectively. (**Table 4**)

Product	**Diamidine units**		**Diacid units**	**Solvent**
	Aromatic protons	CH_3 groups		
47	7.35	1.11	-	CD_3OD
47x2HCl **(47a)**	7.79	1.34, 1.26	-	D_2O
47A_1	7.80 7.79	1.33, 1.26 1.34, 1.26	7.74→7.92, 7.58→7.44 7.52→7.79-7.74 (broad), 7.46→7.63	CD_3OD D_2O
47A_2	7.73 7.78	1.30, 1.24 1.33, 1.25.	8.65→8.46, 8.23→7.94, 7.59→7.32 8.29→8.43, 7.99→8.11, 7.53→7.59	CD_3OD D_2O
47A_3	7.78	1.33, 1.25	7.83→8.03	D_2O
47A_4	7.72 7.70	1.25 1.29, 1.20	8.84→8.72, 8.19→8.13, 7.61→7.47, 4.52→4.46, 1.45→1.42 8.76→8.74, 8.10→8.08, 7.62→7.62, 4.47→4.47, 1.40→1.42	CD_3OD D_2O
47A_5	7.73	1.31, 1.22	8.86→8.88, 8.23→8.24, 7.75→7.78	D_2O
47A_6	7.77	1.33, 1.24	8.33→8.45, 8.06→8.20, 7.89→7.95	D_2O
48x2HCl **(48a)**	7.90	-	-	D_2O
48A_1	7.95	-	7.52→7.44, 7.46→7.39	D_2O
48A_2	7.91	-	8.29→8.23, 7.99→7.95, 7.53→7.50	D_2O
48A_3	7.93	-	7.83 → 7.86	D_2O
48A_4	7.74	-	8.76→8.66, 8.10→8.04, 7.62→7.56, 4.47→4.41, 1.40→1.34	D_2O
48A_5	7.87	-	8.86→8.85, 8.23→8.23, 7.75→7.71-7.80 (broad)	D_2O
48A_4	7.85	-	8.33→8.40, 8.06→8.16, 7.89→7.93	D_2O

Table 4. ^{1}H-NMR chemical shifts for compounds **47A_{1-6}** and **48A_{1-6}**

The modification in the signals position in the case of compound **47A$_1$ is** shown in **Figure 22**. Comparison of the ^{1}H-NMR spectra (in CD_3OD) of diamidine **47**, diacid **A$_1$** and their complex (**47A$_1$**) reveals a deshielding of the signal belonging to the aromatic protons of the diamidine unit together with broadening of the signals.

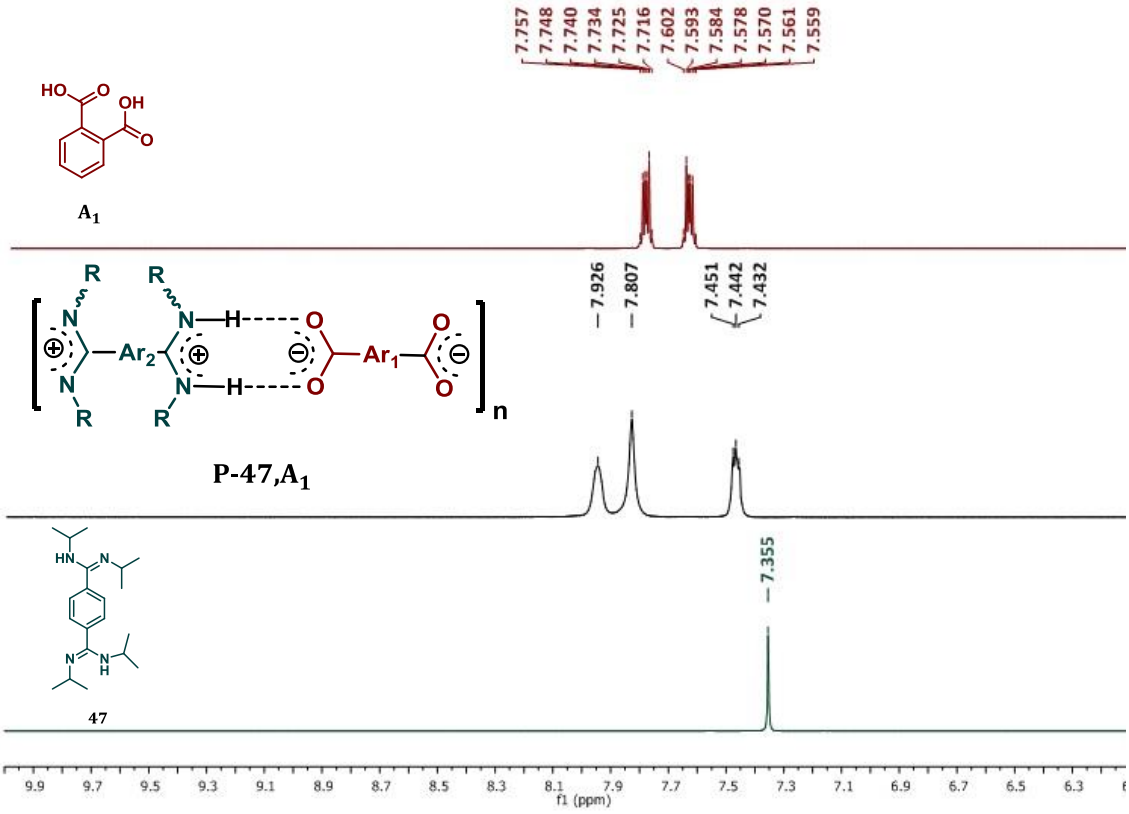

Figure 22. ^{1}H- NMR spectra (CD_3OD) of **47** (bottom), **A$_1$** (top) and **47A$_1$** (middle)

V.3.2 Solid-state investigations

In order to obtain of co-crystals suitable for X-ray diffraction analysis of compounds **47A$_{1\text{-}6}$**, **48A$_{1\text{-}6}$** we applied several crystallization techniques: low temperature, slow evaporation and slow diffusion crystallization. Eight crystals were obtained: **47A$_1$, 47A$_2$**, **47A$_5$**, **47A$_6$**, **48A$_1$, 48A$_2$**, **48A$_5$** and **47A$_6$**. (**Figure 23**) The single crystal structures of these compounds were measured at the University of Montpellier, L'Institut Européen des Membranes, France.

The compound **47A$_1$** crystallized, from Milli-Q water, in the monoclinic space group $P2_1/c$. The asymmetric unit contains half of molecule **47** and a molecule of **A$_1$**, without any water molecules. Each amidine moiety is protonated and, therefore,

dicationic, while the acid **A_1** is in a monoacidic form, with a hydrogen atom shared by the two acidic moieties. Hydrogen bonding association of four **47** and four **A_1** units results in rhombic R^8_8 (54) [36] macrocycle.

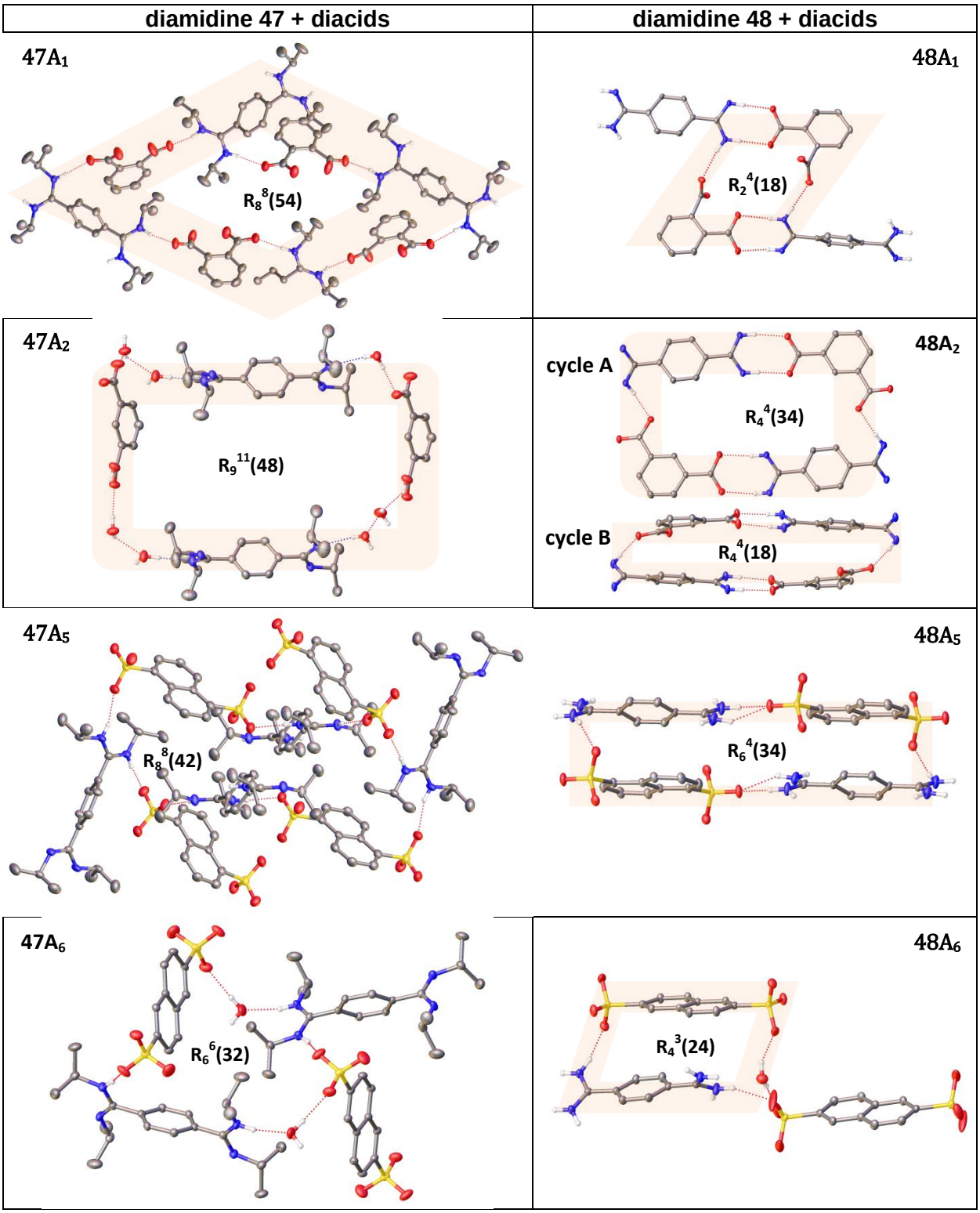

Figure 23. Hydrogen bonding arrays present in crystal structures for **$47A_{1\text{-}2}$**, **$47A_{5\text{-}6}$**, **$48A_{1\text{-}2}$** and **$48A_{5\text{-}6}$** and associated graph-set ($G_d^a(r)$)

[36] Etter, M. C.; MacDonald, J. C.; Bernstein, J. *Acta Cryst. B* **1990**, *46*, 256-262

47A_2 crystallized from Milli-Q water, in the triclinic space group *P*1. The asymmetric unit consists of one molecule of **47**, one molecule of **A_2**, and four molecules of water. The resulted supramolecular 3D structure associated by intermolecular hydrogen bonding amidinium- carboxylate ($^{+}$N-H$\cdots$O^{-}), amidinium-water and carboxylate-water is a rectangular $R_9^{11}(48)$ macrocycle formed by two **47**, two A_2 units and four water molecules.

The N-H bonds of the amidinium groups of a given molecule are systematically *(E, Z)*, thus preventing the expected amidinium-carboxylate synthon (see **Figure 20**) to be formed. Instead, each amidinium moiety interacts with a single carboxylate group through hydrogen bonding. Hydrophobic interactions of the methyl groups and packing of phenyl rings have an important role for the solid state organization. Remarkably, the macrocycles are organised forming supramolecular catenanes. (**Figure 24**) The lattice of this complex consists in chains of such catenanes.

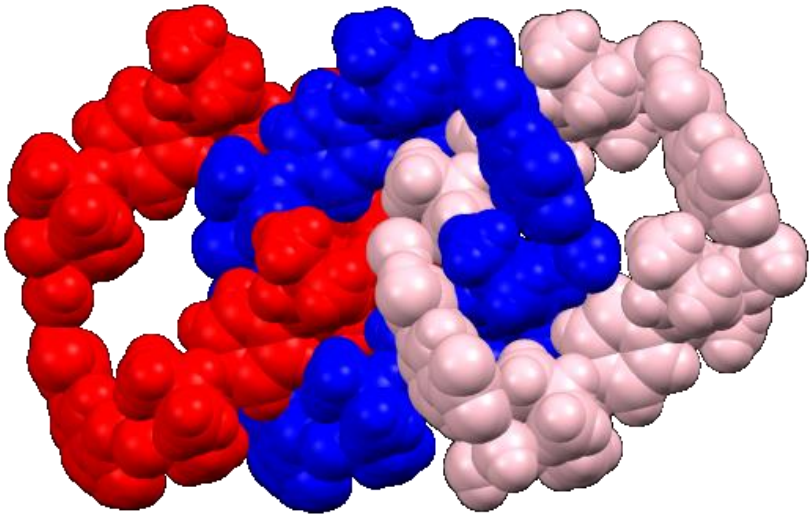

Figure 24. CPK representation of a supramolecular catenane of **47A_2**

47A_5 crystallized, from Milli-Q water, in the monoclinic space group $P2_1/c$. The asymmetric unit contains one molecule of **47** and one molecule of A_5, without water molecules**.** It was observed a rhombic $R^8_8(42)$ macrocycle composed of four molecules of **47** and four **A_5** units through hydrogen bonding. The N-H bonds of the amidinium groups are systematically *(E, Z)*.

47A_6 crystallized, from Milli-Q water, in the monoclinic space group Pbca. The asymmetric unit contains one molecule of **47**, one molecule of **A_6** and one molecule of water. Hydrogen bonding association involving two units of each species **47** and **A_6** results in the formation of a square $R^6_6(32)$ macrocycle. The N-H bonds of the amidinium groups are all *(E, Z)*.

48A_1 crystallized, from Milli-Q water, in the monoclinic space group *Pn*, with symmetrical unit consisting of two molecules of **48**, two molecules of **A_1** and three molecules of water. The *ortho*-orientation of the benzoic-diacid generates a small H-bonding network of rhombic $R_2^4(18)$ shape, involving both dibenzoate molecules and one amidinium moiety of the two benzamidine molecules.

48A_2 crystallizes from mQ water in the triclinic space group *P*1. The asymmetric unit consists of a molecule of **48**, a molecule of **A_2** and five molecules of water. The meta-orientation of the carboxylic groups in this benzoic-diacid generates a larger, rectangular, $R_4^4(34)$, H-bonding network (Cycle 1, **Figure 23**) involving both the acidic groups of two **A_2** molecules and amidinium moieties of two **48** molecules. Interestingly, another rectangular H-bonding motif (Cycle 2, **Figure 23**) including again two molecules of each species, which are this time involved in π-stacking interactions was formed.

48A_5 crystallized, from water in the triclinic space group *P*1, with the symmetrical unit formed from a molecule of **48**, a molecule of **A_5** and one water molecule. A rectangular $R_6^4(34)$ H-bonded macrocycle involving four sulfonic groups of two **A_5** molecules and four amidinium moieties of two **48** molecules was formed.

48A_6 crystallized, from water in the triclinic space group *P*1.The asymmetric units consist of one molecule of **48,** two molecules **A_6** and one molecule of water. A rectangular $R_4^3(36)$ H-bonding network involving two molecules of **A_6**, a molecule of 48 and a water molecule was formed.

V.4 Conclusions

Various molecular associations of the *p*- benzenediamidinium dications (**47**, **48**) with the dianion of dicarboxylic acids (**A_1**-**A_4**), or disulfonic acids (A_5, A_6), were investigated both in solution and solid state. The relative positions of the carboxylic (ortho, meta, para) in **A_1**-**A_4** and the sulfonic group (1,5 or 2,6) influenced the association with the complementary amidinium units.

NMR solution investigations showed significant CAHB associations involved in rapid exchanges.

Studies performed in solid state revealed the formation of macrocycles of various sizes and shapes assembled by hydrogen bonding of the molecular units (*e.g.* **48A$_1$** compared to **48A$_2$**).

The sterical hindrance of the amidine units substituents (*N, N* –diisopropyl) influenced the association behaviour of this compounds that was clearly evidenced in the solid state. Moreover, the preference of the diisopropyl units belonging to the amidine groups for the Z/E configuration was confirmed in solution by NMR experiments.

In the solid state, the formation of the AA-DD motif was observed in few cases (*i.e.* **48A$_1$**, **48A$_2$**) but was not visible on both sides of a symmetrical ditopic molecule.

General Conclusions

This thesis was focused on the design, synthesis, structural characterisation, investigation of the properties and potential applications of tetrasubstituted ligands with tetrahedral and tetragonal orientation of the substituents that contains 9,9'-spirobifluorene and tetraphenyladamantane central units.

Thus, tetrahedral, tetrasubstituted tetraphenyladamantane derivatives that contain cyano, iodo, formyl, carboxy, ethynyl, pyridine and terpyridine functional groups were obtained in good yields. Moreover, the tetraethynyl derivative was further involved in CuAAC click reactions with azide decorated nucleobases (adenine, uracyl, and thymine) to synthesize nucleobases - decorated tetrahedral ligands that are interesting building blocks for hydrogen bonding directed construction of 3D networks.

In addition, 2,2',7,7'-tetrasubstituted-9,9'-spirobifluorene derivatives with tetragonal orientation of the substituents bearing iodo, cyano, pyrimidyl, ethynyl, carboxy and methoxy substituents or nucleobase (uracyl and thymine) units were obtained starting from 9,9'-spirobifluorene. These ligands were further used as molecular units to obtain 2D networks.

Synthesis of 3,3',6,6'-tetrasubstituted-9,9'-spirobifluorene derivatives with tetrahedral orientation of the substituents was also possible by development of a

new and efficient strategy that made use of the orienting effect of the methoxy groups. Thus, the 2,2',7,7'-tetrametoxy-9,9'-spirobifluorene represented a key intermediate to access a large variety of ligands that contain iodo, cyano, formyl, carboxyl, ethynyl, nitro, amino, pyridinyl and thymine substituents at the required positions.

The structures of all ligands were fully characterized by NMR, HRMS, FT-IR, UV-Vis and in some cases by single crystal X-ray diffraction.

The synthesized ligands were used for various applications including the construction of covalent organic frameworks (COFs), metal-organic frameworks (MOFs) and self-assembled architectures.

Thus, tetraphenyladamantane and 9,9'-spirobifluoren ligands containing four iodo or ethynyl reactive groups were used in the construction of 2D and 3D COFs through acetylene coupling or Sonogashira cross-coupling reactions with 1,4-diethynylbenzene or diethynyl-4,4'-biphenyl. These materials were investigated using specific methods and their capacity to adsorb gases such as CO_2 and H_2 was determined as well. Moreover, the catalytic activity of one of these COFs, doped with palladium and gold active metals was studied for the selective hydrogenation of *para*-nitrostyrene.

The metal-ions [*i.e.* Cu(I), Cu(II), Mn(II), Fe(II)] induced association of tetraphenyladamantane ligands with cyano and pyridyl moieties allowed fabrication of MOFs with 3D structures.

Interestingly, the solid state self-assembling of some 3,3',6,6'-tetrasubstituted-9,9'-spirobifluorene derivatives yielded supramolecular architectures of various shapes, exclusively driven by hydrophobic interactions.

Finally, Charge Assisted Hydrogen Bonding (CAHB) associations of *para*-phenylenediamidines with dicarboxylic and sulfonic acids were studied both in solid state and solution. The solid state associations of these compounds revealed the formation of catenanes and marocycles of various shapes.

The results obtained during the PhD thesis were published in 4 ISI articles (3 as main author). Moreover, four other papers are in the final stage of elaboration. The list of the published articles can be found in Appendix.

List of Publications

1. Occurence of Charge-Assisted Hydrogen Bonding in Bis-amidine Complexes Generating Macrocycles
L. Pop, N. D. Hădade, A. van der Lee, M. Barboiu, Y.-M. Legrand, I. Grosu, *Cryst. Growth Des.*, **2016**. (Article ASAP); **DOI:** 10.1021/acs.cgd.6b00246
Impact factor (2015): 4.89

2. Exclusive Hydrophobic Self-Assembly of Adaptive Solid-State Networks of Octasubstituted 9, 9′-Spirobifluorenes
L. Pop, F. Dumitru, N. D. Hădade, Y.-M. Legrand, A. van der Lee, M. Barboiu, I. Grosu, *Org. Lett.*, **2015**, *17*, 3494-3497. DOI: 10.1021/acs.orglett.5b01576
Impact factor (2015): 6.36

3. CuAAC Synthesis of Tetragonal Building Blocks Decorated with Nucleobases
L. Pop, M. L. Golban, N. D. Hădade, C. Socaci, I. Grosu, *Synthesis,* **2015**, *47*, 2799-2804. DOI: 10.1055/s-0034-1378782
Impact factor (2015): 2.69

4. Novel Nucleobase-Decorated Tripodands: Synthesis and Supramolecular Properties
M. Golban, V. Paşcanu, N. D. Hădade, **L. Pop**, C. Socaci, I. Grosu, *Synthesis,* **2014**, *46*, 1229-1235. **DOI:** 10.1055/s-0033-1340833
Impact factor (2014): 2.69